

SLAC-156  
(TH) and (EXP)  
UC-34

EIKONAL METHODS AND ABSORPTIVE EFFECTS  
IN HADRONIC PRODUCTION PROCESSES\*

THOMAS L. NEFF

STANFORD LINEAR ACCELERATOR CENTER

STANFORD UNIVERSITY

Stanford, California 94305

PREPARED FOR THE U. S. ATOMIC ENERGY  
COMMISSION UNDER CONTRACT NO. AT(04-3)-515

PET  
249

September 1972

~

Printed in the United States of America. Available from National Technical Information Service, U. S. Department of Commerce, 5285 Port Royal Road, Springfield, Virginia 22151.  
Price: Printed Copy \$3.00; Microfiche \$0.95.

---

\*Ph. D. Dissertation.

## ABSTRACT

Absorptive effects are shown to be of utility in probing the nature of hadronic interactions and in testing models for multiple production. These effects result theoretically from the imposition of full  $s$ -channel unitarity upon model assumptions which do not possess it, and reflect the influence of small-scale (in configuration space) hadron dynamics. The globally smooth properties of hadronic production (scaling, Poisson multiplicities, etc.) are the result of the innumerable competitive mechanisms involved in a complex many-body problem. The local dynamics is reflected in small effects in certain experimental distributions. These effects and others are illustrated in a heuristic parton model which establishes the connection between multi- and poly-peripheral production mechanisms, the eikonal approximation and the nature of strong absorption. The strong cuts which are required by unitarity arise from the interplay between large distance (Regge) and small distance (non-Regge) dynamics. The usual non-relativistic treatment of absorption is extended to the relativistic domain and the new features discussed. Divers mechanisms for hadronic production are then taken as Born terms to be unitarized by absorption and the experimental consequences explored. The large transverse momentum region is appreciably enhanced and relative momentum (and angular) correlations result. Comparison is made with experiment.

## PREFACE AND ACKNOWLEDGEMENT

Some of the material presented in sections VI and VII has been published.\* The continual encouragement and critical guidance of R. Blankenbecler throughout this research is deeply and humbly appreciated. His ability to preserve, clarify and build upon good ideas while letting the bad die gracefully make him an ideal advisor and a model of research integrity. I also wish to thank my past and present colleagues, particularly C. E. Carlson, R. Savit, R. Jaffe and S. Brodsky for their friendship. Particular appreciation is due S. D. Drell, whose personal qualities are directly responsible for the stimulating, noisy, openness which makes the SLAC theory group a uniquely rewarding place to work.

\*R. Blankenbecler and T. L. Neff, Phys. Rev. D5, 128 (1972)  
T. L. Neff, R. Savit, and R. Blankenbecler, Phys. Letters 38B, 515 (1972)

## TABLE OF CONTENTS

I.	Introduction . . . . .	1
II.	Strong Absorption . . . . .	15
III.	Parton Model . . . . .	21
IV.	Re-Born . . . . .	33
V.	Absorption and Relativistic Eikonal . . . . .	38
VI.	Construction of Models . . . . .	52
VII.	Azimuthal Distributions and the Geometry of Production . . . . .	83
VIII.	Conclusion . . . . .	93
	References . . . . .	97

## LIST OF ILLUSTRATIONS

1.	Born term "B" and contributions to elastic scattering . . . . .	16
2.	Impact representation for $T_{el}$ . . . . .	16
3.	Born term "C" and contributions to $T_{el}$ . . . . .	17
4.	Absorptive prescription . . . . .	20
5.	Multiperipheral parton diagram . . . . .	22
6.	Connected walk in the transverse plane . . . . .	24
7.	Diagrams yielding ordinary cuts of diverse nature	26
8.	Strong absorption and extraordinary cuts . . . . .	27
9.	Overlaps in the transverse plane . . . . .	28
10.	Eikonal interpretation of parton model . . . . .	31
11.	Leading particles and vertex structure . . . . .	35
12.	Impact parameter representations and Fourier transforms . . . . .	49
13.	Model constructions . . . . .	62
14.	Experimental longitudinal distributions for $\pi^+p \rightarrow \pi^+\pi^+n$ at 16 GeV/c . . . . .	63
15a.	Experimental distribution in relative transverse momentum between leading particles in same . . . . .	64
15b.	Experimental distribution in relative transverse momentum between leading nucleon and secondary pion . . . . .	65
15c.	Experimental distribution in transverse momentum of leading nucleon . . . . .	66
15d.	Experimental distribution in transverse momentum of secondary pion . . . . .	67
16a.	Predictions of absorbed multiperipheral model for the distribution in $v^2$ in the $2 \rightarrow 3$ reaction. The dotted line indicates no absorption, the dashed real absorption, while the solid line is for complex absorption . . . . .	68

16b.	Distribution in $v^2$ from absorbed multiperipheral model for reaction $2 \rightarrow 4$ . . . . .	68
17a.	Predictions of iterative production model for distribution in $w^2$ for $2 \rightarrow 4$ reaction . . . . .	69
17b.	Prediction of multiperipheral model for distribution in $w^2$ for $2 \rightarrow 4$ reaction . . . . .	69
18.	Eikonal graphs whose contributions can cancel in the multiregge region of phase space . . . . .	76
19.	Fragmentation model . . . . .	79
20.	Qualitative features of transverse momentum distributions in the fragmentation models . . . . .	82
21a.	Multiperipheral configuration . . . . .	85
21b.	Pion radiation from overlap in transverse configuration space . . . . .	85
21c.	Monopole and dipole radiation patterns. Dotted line is with no absorption, solid curve results when absorptive effects are included . . . . .	85
22a.	Azimuthal distributions in the $\pi p$ and $Kp$ reactions. The dashed line is a best fit assuming the phenomenological parameter $c=0$ (no absorption) while the dotted line is the absorptive model prediction . . . . .	87
22b.	Cartesian-correlation plot for the $\pi p$ reaction as functions of $\pi_x^+$ and $\pi_y^+$ , where $\pi^+$ is the secondary particle and the x-axis is defined by the transverse momentum of the leading boson. The dotted line is for no absorption . . . . .	88
22c.	Cartesian-correlation plot for the $Kp$ reaction as functions of $\pi_x$ and $\pi_y$ , where $\pi$ is the secondary particle and the x-axis is defined by the transverse momentum of the leading boson (the kaon) . . . . .	89

## INTRODUCTION

Hadronic interactions are a source of continuing inspiration and frustration to theoreticians. One's certain knowledge of purely hadronic processes is slight and usually reduces to a few global experimental observations. These include the boundedness of transverse spectra, approximate scaling or limiting fragmentation, and the relationship between energy dependences and quantum number symmetries. Models nearly always incorporate these global features from the beginning.

Two-body and quasi-two-body reactions have received very detailed phenomenological treatment in both exchange and direct channel representations. One would like to utilize the knowledge gained from two-body reactions to build models for production amplitudes. There are the global constraints on such a task mentioned above, and then the further constraint of s-channel unitarity in relating production amplitudes to elastic scattering. The simultaneous satisfaction of these conditions is a difficult matter. One way out, of course, is to break the problem up into two components--into diffractive and non-diffractive contributions. This is particularly convenient in an

exchange picture, but can lead to great pathologies if one treats Pomeron and ordinary Reggeons on the same footing.<sup>1</sup> This is not to say that the study of pathology is unrewarding. An alternative is the dual absorptive approach of Harari and others: Diffractive scattering is geometrical, while ordinary exchanges are dual to direct channel resonance dynamics.<sup>2</sup>

It is a truism that hadronic interactions involve composite structures of high complexity. Models vary as to the organization of that complexity--from fragmentation and parton models which emphasize the role of s-channel composites, to Regge poles which one believes to represent the exchange of t-channel composites with rising spectra. In contrast, eikonal models divorce the many-body complexity, for elastic scattering at least, from the asymptotic particles and, in effect, invest it in a smooth medium with pleasing optical properties.

In constructing models for production amplitudes one can take several points of view, resulting in multiperipheral or multi-Regge, diffractive fragmentation (fireball, jet, Nova, etc.) and dual models. The diffractive models sometimes have an added pionization or "pulverization" component. We

will later add a model which might be called poly-peripheral in that successive multiperipheral chains of small multiplicity occur iteratively in the s-channel. All of these models involve strong simplifying assumptions of incoherence and statistical independence in the form of factorization properties, lack of long-chain correlations and, in the case of the the diffractive fragmentation model, factorization of the pomeron and subsequent independent decay of the heavy resonances produced. Such models can be constructed for particular exclusive channels but most are either applied only to inclusive reactions in which one or two particles are detected or are used to calculate global quantities such as mean multiplicity.

Experimental tests of the different dynamical assumptions involved in these models are difficult to come by. Global predictions are hard to test experimentally in the few regions which are model dependent. Scaling in the pionization region is an example. Correlations have thus been a subject of much contemporary interest.<sup>3</sup>

The formulation of the discussion of correlations is usually based on a direct transcription of the configuration space intuition developed in solid

state (or fluid) physics into the momentum space of multi-particle states.<sup>4</sup> Wide separation, in the space of either problem, should, by common inspiration, mean lack of dynamical connection. Models for hadronic interactions nearly universally incorporate the factorization properties which insure such momentum space behaviour. It shall be one of our major concerns to investigate the validity of this transcription and the factorization properties of the model constructions resulting from it. In this regard, we note that the (explicitly unitary) eikonal models dynamically connect disjoint regions of phase space.

One of the major problems in studying dynamical effects by correlation techniques is the necessity of separating those which are solely a result of conservation laws. One of the most restrictive constraints in inclusive reactions, for example, is energy-momentum conservation. The correlation function description taken from solid state physics (where momentum is not conserved) does not eliminate these kinematic correlations and it is difficult to separate those correlations which are due to dynamical assumptions from those which are not. For example, many sum rules based on conservation laws have been derived which are interpreted as tests of model

assumptions. These constraints are non-trivial only when applied to inclusive reactions.<sup>5</sup>

It would be even more useful to devise correlation functions which eliminate the trivial correlations due to the constraint on phase space imposed by momentum conservation. Then the introduction of a dynamical assertion would have more obvious consequences than that it satisfies momentum conservation.

To this end, consider the exclusive process  $a + b \rightarrow n$  identical final state particles.<sup>6</sup> Let the matrix element have the simple "peripheral phase space" form

$$|\langle P_a P_b | T | p_1 \dots p_n \rangle|^2 = g(s) \prod_{i=1}^n f(p_{i\perp}^2) \quad 1.1$$

The function  $g(s)$  is necessary to adjust the  $s$ -dependence of the total cross section to the desired form. The functions  $f$  give simple results in two cases. The first is pure phase space with  $f = \text{constant}$ . The second is the peripheral phase space above with the  $f$ 's strongly damping the transverse momenta (e.g. exponential or Gaussian). This form is invariant only under boosts along the collision axis. If  $P = P_a + P_b$  and  $s = P^2$ , the exclusive cross section has the form

$$\frac{d\sigma}{dP_1 \dots dP_n} = \frac{(2\pi)^4}{2\lambda(s, m_a^2, m_b^2)} |\langle P_a P_b | T | P_1 \dots P_n \rangle|^2 \delta^{(4)}(P - \sum_i P_i) \quad 1.2$$

where  $\lambda^2(x, y, z) = x^2 + y^2 + z^2 - 2xy - 2xz - 2yz$ . The total cross section is

$$\sigma_{\text{tot}}(s) = \sum_{n=0}^{\infty} \frac{1}{n!} \int dP_1 \dots dP_n \frac{d\sigma}{dP_1 \dots dP_n} \quad 1.3$$

where  $dp = d^3p / ((2\pi)^3 2E)$ .

To determine the normalization of  $\sigma_{\text{tot}}$ , the integrals over phase space must be done. Suppose we require that  $s^m \sigma_{\text{tot}} = \text{constant} = c$ . In the case  $f = \text{constant} = a$ , the phase space integrals can be done<sup>7</sup> if all masses are neglected:

$$(2\pi)^4 \prod_{i=1}^n \left[ \int \frac{d^3p_i}{2p_i (2\pi)^3} \right] \delta^{(4)}(P - \sum P_i) = \frac{s^{n-2}}{8 (16\pi^2)^{n-2} (n-1)! (n-2)!} \quad 1.4$$

The requirement then is that

$$c = s^m \sigma_{\text{tot}} = \frac{g(s) s^m}{2\lambda(s)} \leq \frac{a^n s^{n-2}}{8 (16\pi^2)^{n-2} n! (n-1)! (n-2)!} \quad 1.5$$

Summing the series determines the function  $g(s)$  and the constant  $a$  in terms of  $c$  and  $m$ . There may be many

solutions. In general, the choice of solution can be fixed by the  $s$ -dependence of the elastic cross section. We absorb the energy dependences into the kinematic factor, defining a new function  $\bar{\lambda}(s)$ . More interesting is the peripheral phase space function, where if we ignore the  $p_{\perp}^2$  dependence and the masses (setting  $f(0)=a$ ), the result is

$$\sigma_n = \text{const.} \frac{g(s) a^n (\ln s)^{n-2}}{s \lambda(s, m_a^2, m_b^2) (n-2)!} \quad 1.6$$

so that

$$\sigma_{\text{tot}} = \frac{g(s) a^2}{s \lambda(s)} s^a \quad 1.7$$

The simplest choice is  $a=1$ ,  $g(s)=s$ , giving an elastic cross section which falls as  $1/s$  and a constant total cross section. Again this dependence may be absorbed into the new function  $\bar{\lambda}(s)$ .

The  $k$ -particle inclusive cross section is

$$\frac{d\sigma_{in}}{dp_1 \dots dp_k} = \sum_{n=k}^{\infty} \frac{1}{(n-k)!} \int dp_{k+1} \dots dp_n \frac{d\sigma}{dp_1 \dots dp_n} \quad 1.8$$

Introducing our peripheral matrix element,

$$\frac{d\sigma_{in}}{dp_1 \dots dp_k} = \frac{C}{\bar{\lambda}(s)} \left[ \prod_{i=1}^k f(p_{i\perp}^2) \right] \sum_{n=k}^{\infty} \frac{1}{(n-k)!} \int dp_{k+1} \dots dp_n \left[ \prod_{i=k+1}^n f(p_{i\perp}^2) \right] \cdot \delta^{(4)} \left[ (P - \sum_{i=1}^k p_i) - \sum_{i=k+1}^n p_i \right] \quad 1.9$$

where C = constant . Let  $p_{\perp} = 0$  and define  $\bar{P} = P - \sum_{i=1}^k p_i$ .  
 Changing the dummy indices and putting  $\bar{P}^2 = \bar{s}$ , we obtain

$$\begin{aligned} \frac{d\sigma_{in}}{dp_1 \dots dp_k} &= \frac{\bar{\lambda}(\bar{s})}{\bar{\lambda}(s)} \prod_{i=1}^k f(p_{i\perp}^2) \left\{ \frac{C}{\bar{\lambda}(\bar{s})} \sum_{n=0}^{\infty} \frac{1}{n!} \int dk_1 \dots dk_n \prod_{i=1}^n f(k_{i\perp}^2) \delta^{(4)}(\bar{P} - \sum_{i=1}^n k_i) \right\} \\ &= \frac{\bar{\lambda}(\bar{s})}{\bar{\lambda}(s)} \left[ \prod_{i=1}^k f(p_{i\perp}^2) \right] \sigma_{tot}(\bar{s}) \end{aligned} \quad 1.10$$

Now define

$$\frac{d\Sigma_{in}(P)}{dp_1 \dots dp_k} \equiv \frac{\bar{\lambda}(s)}{\bar{\lambda}(\bar{s}) \sigma_{tot}(\bar{s})} \frac{d\sigma_{in}}{dp_1 \dots dp_k} = \prod_{i=1}^k f(p_{i\perp}^2) \quad 1.11$$

This is a cross section normalized to the kinematic factor and total cross section corresponding to the phase space volume remaining when the k vectors  $p_1 \dots p_k$  have been chosen-- that is, at energy  $\bar{s}$  . We now use these new quantities to define correlation functions

$$\tilde{\rho}_P^{(k)}(p_1 \dots p_k):$$

$$\begin{aligned}
\tilde{\rho}_P^{(1)}(p_1) &\equiv \frac{dZ(p)}{dp_1} = f(p_{1L}^2) \\
\tilde{\rho}_P^{(2)}(p_1, p_2) &\equiv \frac{dZ(p)}{dp_1 dp_2} - \tilde{\rho}_P^{(1)}(p_1) \tilde{\rho}_P^{(1)}(p_2) = 0 \\
\vdots & \qquad \qquad \qquad \vdots \qquad \qquad \qquad \vdots
\end{aligned}
\tag{1.12}$$

All higher correlation functions vanish. It is easy to write these functions in terms of the more commonly normalized functions  $\rho_P^{(k)}(p_1, \dots, p_k)$  where

$$\begin{aligned}
\rho_P^{(1)}(p_1) &= \frac{d\sigma_{in}}{dp_1} \\
\rho_P^{(2)}(p_1, p_2) &= \frac{d^2\sigma_{in}}{dp_1 dp_2} - \frac{d\sigma_{in}}{dp_1} \frac{d\sigma_{in}}{dp_2}
\end{aligned}
\tag{1.13}$$

The result for  $\tilde{\rho}_P^{(2)}$  in terms of  $\rho^{(1)}$  and  $\rho^{(2)}$  is

$$\tilde{\rho}_P^{(2)}(p_1, p_2) = \frac{A(s)}{A(s_{12})} \left\{ \left[ 1 - \frac{A(s)A(s_{12})}{A(s_1)A(s_2)} \right] \rho_P^{(1)}(p_1) \rho_P^{(1)}(p_2) + \rho_P^{(2)}(p_1, p_2) \right\}
\tag{1.14}$$

where

$$\begin{aligned}
s_1 &= (P - p_1)^2 \\
s_2 &= (P - p_2)^2 \\
s_{12} &= (P - p_1 - p_2)^2
\end{aligned}
\tag{1.15}$$

and  $A(s) \equiv \bar{\lambda}(s) \sigma_{tot}(s)$ . When  $p_1$  and  $p_2$  are in the pionization region, where  $s_1 \approx s_2 \approx s_{12} \approx s$ , the factor in braces tends to vanish and  $\tilde{\rho}^{(2)}$  is very nearly  $\rho^{(2)}$ . For  $p_1$  and  $p_2$  in opposite fragmentation regions  $\tilde{\rho}^{(2)}$  and  $\rho^{(2)}$  are in general quite different--  $\tilde{\rho}^{(2)}$  vanishes while  $\rho^{(2)}$  does not. <sup>8</sup>

We now consider a model amplitude with a dynamical input which leads to a non-vanishing correlation for some distributions. Write the amplitude for a simple two-fireball model in the center-of-mass with transverse momentum transfer  $\vec{\Delta}_\perp$  as

$$\langle p_a p_b | T | p_1 \dots p_{N_1}; q_1 \dots q_{N_2} \rangle = g(s) \beta(\Delta) \prod_{i=1}^{N_1} f^{1/2}(p_{i\perp}^2) \prod_{j=1}^{N_2} g^{1/2}(q_{j\perp}^2) \quad 1.16$$

where  $\vec{\Delta}_\perp = \sum_{i=1}^{N_2} \vec{q}_{i\perp} = -\sum_{j=1}^{N_1} \vec{p}_{j\perp}$ , so that

$$\begin{aligned} \sigma_{\text{tot}}(s) &= \frac{C}{\lambda(s)} \sum_{N_1} \sum_{N_2} \frac{1}{N_1! N_2!} \prod_{i=1}^{N_1} \left[ \int d p_i f(p_{i\perp}^2) \right] \prod_{j=1}^{N_2} \left[ \int d q_j g(q_{j\perp}^2) \right] \cdot \\ &\quad \cdot \beta^2(\sum \vec{q}_{i\perp}) \delta^{(4)}(P - \sum p_i - \sum q_j) \end{aligned} \quad 1.17$$

Now consider the two-particle inclusive distribution for two right-movers:

$$\begin{aligned} \frac{d\sigma_{in}}{d p_1 d p_2} &= \frac{C}{\lambda(s)} f(p_{1\perp}^2) f(p_{2\perp}^2) \sum_{N_1=2}^{\infty} \sum_{N_2=0}^{\infty} \frac{1}{(N_1-2)! N_2!} \prod_{i=3}^{N_1} \prod_{j=1}^{N_2} \left[ \int d p_i d q_j f(p_{i\perp}^2) g(q_{j\perp}^2) \right] \cdot \\ &\quad \cdot \beta^2(\sum_{i=1}^{N_2} \vec{q}_{i\perp}) \delta^{(4)}(\vec{p} - \sum_3^{N_1} p_i - \sum_1^{N_2} q_j) \end{aligned} \quad 1.18$$

The "diffractive" exchange function  $\beta$  is thus independent of  $p, p_2$  so we can again extract  $\sigma_T(\hat{s})$  and write

$$\frac{d\Sigma_{in}}{dP_1 dP_2} = \frac{\bar{\lambda}(s)}{\lambda(s)\sigma_T(s)} \frac{d\sigma_{in}}{dP_1 dP_2} = f(P_{1\perp}^2) f(P_{2\perp}^2) \quad 1.19$$

Again, the two-particle correlation  $\tilde{\rho}_P^{(2)}(P_1, P_2)$  vanishes. There is no dependence upon  $\vec{p}_1, \vec{p}_2$  induced by the diffractive exchange.

The correlation  $\tilde{\rho}_P^{(2)}(P_1, q_1)$  between right and left moving fragments, however, is a very different story. We write

$$\begin{aligned} \frac{d\sigma_{in}}{dP_1 dq_1} &= \frac{c}{\lambda(s)} f(P_{1\perp}^2) g(q_{1\perp}^2) \sum_{N_1=1}^{\infty} \sum_{N_2=1}^{\infty} \frac{1}{(N_1-1)! (N_2-1)!} \\ &\quad \cdot \prod_{i=2}^{N_1} \prod_{j=2}^{N_2} \left[ \int dP_i dq_{ij} f(P_{i\perp}^2) g(q_{ij\perp}^2) \right] \cdot \\ &\quad \cdot \beta^2 \left( \frac{\vec{q}_1 - \vec{P}_1}{2} + \frac{\sum_{i=2}^{N_2} \vec{q}_i - \sum_{i=2}^{N_1} \vec{P}_i}{2} \right) \delta^{(4)} \left( \vec{P} - \sum_{i=2}^{N_1} \vec{P}_i - \sum_{j=2}^{N_2} \vec{q}_j \right) \end{aligned} \quad 1.20$$

where  $\vec{P} = P - p_1 - q_1$ . It is now difficult to extract  $\sigma_T(s)$  unless  $(\vec{q}_1 - \vec{P}_1)_\perp = 0$ , or the function  $\beta$  is cleverly chosen. We therefore write

$$\frac{d\sigma_{in}}{dP_1 dq_1} = f(P_{1\perp}^2) g(q_{1\perp}^2) \frac{\bar{\lambda}(s)\sigma_T(s)}{\lambda(s)} \gamma(s; (\vec{q}_1 - \vec{P}_1)_\perp^2) \quad 1.21$$

where  $\gamma(s, (\vec{q}_1 - \vec{P}_1)_\perp^2 = 0) = 1$  and  $\tilde{s} = (P - p_1 - q_1)^2$ . This implies that the two-particle correlation function

$$\tilde{\rho}_p^{(2)}(p, q) = \left[ 1 - \gamma(\vec{S}; (\vec{p}_1 - \vec{q}_1)_\perp^2) \right] \cdot f(p_{1z}) g(q_{1z}) \quad 1.22$$

is in general nonvanishing. There are thus non-trivial azimuthal correlations resulting from the assumption of a particular production mechanism. Here, the correlation will be largest when the particles do not have the same direction in transverse space. This negative transverse angle correlation has dynamical meaning. Anticipating, we note that if this distribution in  $(\vec{q}_1 - \vec{p}_1)_\perp$  is Fourier transformed into the conjugate impact parameter space, the correlation structure comes from the small distance behaviour of the exchange mechanism. The large-scale behaviour is related to the smooth phase-space-like part of the distribution with vanishing correlations. This statement will be shown to be more generally true. The small distance dynamics may be studied by transverse momentum correlations if they are properly defined.

It has been commonly believed<sup>9</sup> that the experimental two-particle azimuthal distributions are given by "pure" phase space. If this is strictly true, any model which changes the peripheral phase space result of vanishing  $\tilde{\rho}^{(k)}(k > 1)$  will be wrong--including

the one above. What is more likely true is that hadron dynamics makes only slight modifications in the phase space distributions globally even though the local (short distance) dynamics may be strong. This is a not unusual feature of very complicated many-body systems where numerous competing mechanisms produce smooth averages for certain quantities, but not (fortunately) for others. We shall see, from several points of view, how this might come about.

The preceding discussion is of course deeply connected with another constraint on production amplitudes-- the imposition of full s-channel unitarity. Much of this discussion will be phrased in the language of absorption in an impact parameter representation for production amplitudes. In the following sections we will explore, by means of simple example, the origin and necessity for strong absorption (or cuts). This discussion would equally well apply to two-body reactions, but the production of the single secondary in the  $2 \rightarrow 3$  reaction is shown to open up kinematic degrees of freedom which allow more complete study of the small distance, or higher Fourier components, of the interaction. The simple example is then extended to a parton model which allows us to establish the connection between eikonal behaviour and

the exchange mechanisms. The resulting cuts are of two different types. It is also possible to develop heuristically the relationship between longitudinal and transverse spectra. For a more detailed discussion of this connection we then return to the simple example for a discussion of kinematics and other matters.

This is followed by an extension to the relativistic domain of the non-relativistic prescriptions for absorption. A number of possible circumstances and reactions are treated by use of the relativistic eikonal approximation. Impact parameter representations are discussed and spin effects considered. In the last sections we construct absorbed multiparticle production amplitudes of several types and compare with experiment.

## II. STRONG ABSORPTION

We now wish to consider the general problem of unitarizing a given multiparticle amplitude, and in particular the formal possibility of strong absorption (strong cuts) in an absorptive prescription. The general belief is that a given exclusive inelastic channel amplitude should have vanishing significance as a collision becomes more central due to the presence of more and more inelastic channels opening up.

Care must be taken in formulating this statement, however. One might expect that one should simply multiply a given Born term (a multiperipheral chain for example) by a function  $S(s,b)$  which vanishes at  $|b|=0$ , forcing the given amplitude to vanish. We show, by means of an example, that the assumption of a given Born term as the production mechanism can lead to the necessity for an "over-absorptive" prescription, or a function  $S(s,b)$  which has finite value at  $b=0$  and may even have changed sign.

Suppose first the simple case in which there is but one mechanism for particle production, with a multiperipheral Born term "B" as in fig. 1.a. This term makes a contribution to the elastic eikonal

T-matrix,  $T_{el}^{(B)}(b)$ , as shown in fig 1b, where there is an

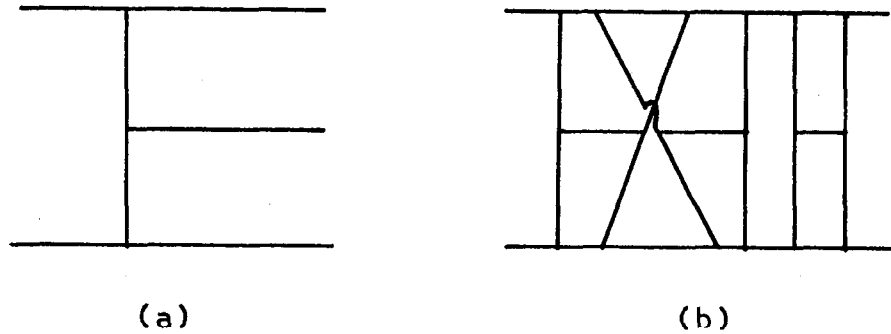


Fig. 1

implied eikonal sum over all such Feynman graphs. If this is the only interaction, we have

$$S_{el}^{(B)} = 1 - iT_{el}^{(B)} \quad 2.1$$

and we would then write the eikonal absorption-corrected amplitude in the usual way as

$$\text{Amp}_{2 \rightarrow 3} \approx B \cdot S_{el}^{(B)} \quad 2.2$$

In an ideal world at least,  $T_{el}$  is purely imaginary and with the impact parameter form usually attributed to the Pomeron,<sup>10</sup> as in fig 2.a,b.

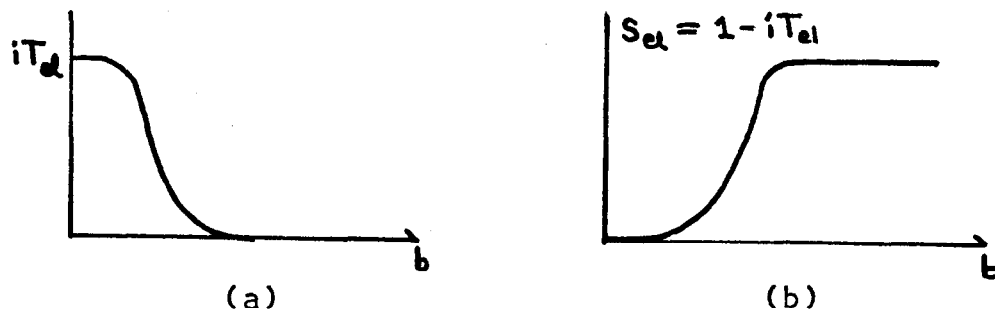


Fig. 2

In this case, the elastic S-matrix absorption factor will agree with what is expected by the usual argument; it vanishes at  $|\vec{b}|=0$ .

However, suppose there is another possible mechanism for production into the same channel. For example, the new Born term "C" of fig. 3a. In general, C will be of shorter range than B.

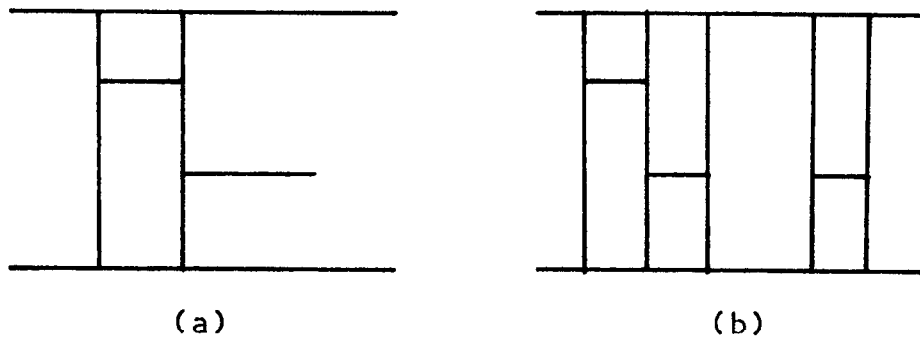


Fig. 3

The contributions to  $T_{el}$ , which come from both B and C, are more complicated, as shown. This is now the Pomeron, since  $T_{el}$  must include the shadows of both production mechanisms. The absorbed single-particle production amplitude is now

$$Amp_{2 \rightarrow 3} = (B+C) S_{el}^{(B,C)} = (B+C) (1 - iT_{el}^{(B,C)}) \quad 2.3$$

The crucial point is that if we don't know about C and assume only B as a Born term, the absorptive factor must change if it is to unitarize this truncated Born approximation. That is, we want to know  $S'(s, \vec{b})$  such

that

$$(B+C)S'_a \approx B \cdot S' \quad 2.4$$

There is no correct prescription for  $S'$ , given our lack of knowledge of all production mechanisms. Suppose, however, we assume we know  $T_a$  as given, for example, by fig. 2(a). and then write

$$S' \equiv 1 - i\lambda T_a \quad 2.5$$

where the parameter  $\lambda$  adjusts for all the competing mechanisms leading to the same final state which we are ignoring when we use only B. At finite energies, there is no reason to believe that  $\lambda$  is real (if we write  $T_a$  as pure imaginary) since there are many processes available which give an experimentally observed real part to  $T_a$ . The relationship between  $\text{Re } \lambda$  and  $\text{Im } \lambda$  is almost certainly s-dependent, reflecting the changing magnitude of the real part of  $T_a$ . This will turn out to have consequences for polarizations and other effects in absorbed inelastic reactions. The energy dependence is probably quite slow, perhaps logarithmic. There is, in general, no constraint on how large  $\lambda$  may become. Phenomenological fits to two-body inelastic

reactions indicate that when strong cuts are required,  $\lambda$  is about 2.<sup>11</sup> In general,  $\lambda$  will be a function of  $b$ . The form chosen for absorption, we hasten to repeat, is just a recipe, like every other prescription, chosen for ease of calculation in what follows.

The usual geometrical interpretation of absorption in, for example, an exchange model (single particle or Regge) is that the single exchange overweights the small impact parameter region and a sharper edge in configuration space is needed to sharpen the forward peak. The presence of other channels thus leads to a black disc from which scattering occurs. One must invent a cancelling shadow wave, out of phase with the incident wave and of the same modulus at  $b=0$ , with the disc region as source.

In the overabsorptive case ( $\lambda > 1$ ), the sharpening of the forward peak will in general be greater since the edge moves out in  $b$  and becomes sharper (see figure 4) in profile. The absorptive factor vanishes at  $b > 0$  and at even smaller  $b$ , the prescription indicates that the shadow wave overcompensates. More precisely, there are two kinds of shadow-- those of B and C. The shadow wave of mechanism C interferes with the direct wave from mechanism B to produce more large angle scattering than

otherwise.

It is clear that where the absorptive effects are to be largest and have the greatest sensitivity to the dynamics is at small distances. It is just this fact that will allow tests of model assumptions. In the next section, the problem of small distance structure and the origin of strong cuts is illustrated in a revealing, but typically mechanistic, parton model.

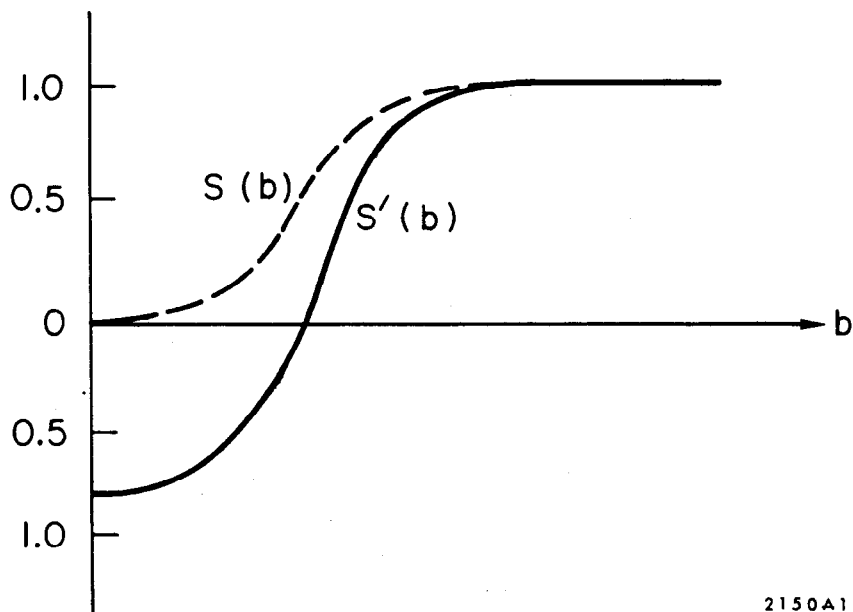


Fig. 4

### III. PARTON MODEL

We now proceed to generalize the Born term discussion above to a parton construction analogous to that developed in Q.E.D. models. The use of field theory models has an honorable history in the study of Regge cuts.<sup>12</sup> What little we know about these singularities has come from such analysis. In the parton model analysis we will show not only how the more common AFS and Mandelstam<sup>12</sup> cuts arise from the kinematic overlap of large scale composite structures but also how new cuts can arise at the deeper dynamical level of small scale structures. There will be sufficient freedom to adapt this heuristic approach to all of the production mechanisms mentioned above in a way which reveals their defects. The origin of the eikonal approximation will be particularly interesting.

Consider first the multiperipheral diagram of figure 5, where the line lengths represent the longitudinal momenta (or fractions thereof) carried by the partons in the center of mass. A longitudinal boost moves the central region toward the slower particle. If we suppose that the virtual partons have a common rest frame lifetime  $\tau_0$ ,<sup>13</sup> then the fast partons will have a center of mass time-dilated lifetime before

cascading, very large compared to that of a slow parton. If in addition the transverse momentum

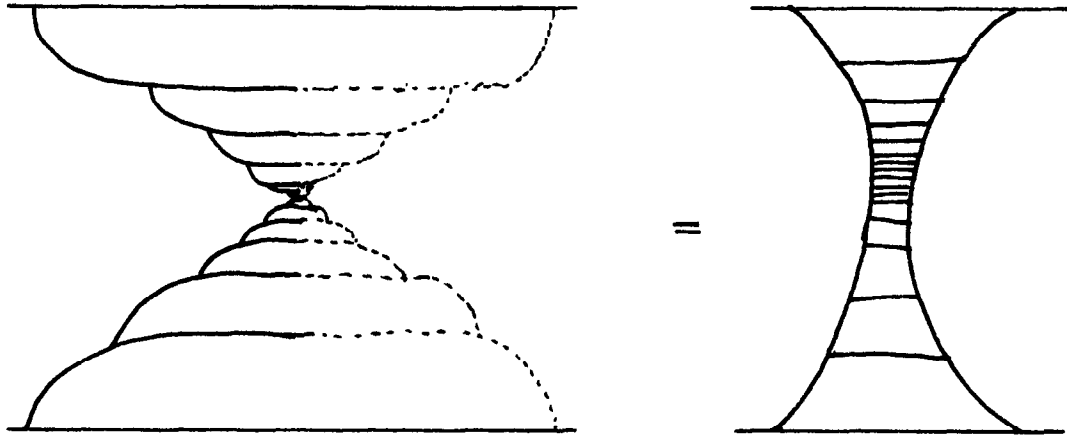


Fig. 5

transfer at each point in the cascade is cut off at the usual characteristic value  $\langle k_{\perp} \rangle \approx 0.3-0.4$  GeV, then the slower partons will step off a smaller transverse distance before decaying. We have also assumed damping in the longitudinal momentum transfer.

If we consider the first few steps, we can use the infinite momentum "energy" denominator to estimate the transverse configuration space spread of the walk. For adjacent partons with longitudinal fractions  $x_i$  and  $x_{i+1}$ , the two-particle free Green's function gives a dependence of

$$G_0^{(x_i)} \approx K_0 \left( \sqrt{\frac{\langle m_{i\perp}^2 \rangle}{x_i} + \frac{\langle m_{i+1\perp}^2 \rangle}{x_{i+1}}} \cdot b_{i\perp} \right)$$

where  $\langle m_{\perp}^2 \rangle = \langle m^2 + k_{\perp}^2 \rangle$ . The function  $K_0$  falls exponentially for moderate and large values of its argument. Hence the partons carrying large fractions of the incident momentum are spread out in transverse configuration space. The density of longitudinal momentum per unit area is thus likely to be low. Forgetting about linking up the chain to the other external particle chain (which would only constrain the end) we thus have, for each hadron, a transverse random walk of decreasing step length. The step length depends upon the relative subenergy of the adjacent partons.

This mathematical argument fails, of course, for the central or wee region but the essential features are clear. The wee region will be considered as beginning with longitudinal fractions of order  $1/\sqrt{s}$  since this is the characteristic center of mass collision time with which the parton lifetime should be compared. The central region should probably not, and for this same reason, be regarded as identifiable with either incoming hadron. A simple way to rephrase this point is to say that the high energy incoming particles polarize the hadronic vacuum, which has a very quick relaxation time. The central region which exists only during the short collision time is the result of mutual

excitation by both particles. The random walk character is thus altered but primarily in the fast parton region. The wee walk doesn't go very far and can thus maintain the Poisson character which can give logarithmic multiplicities. The first few fast parton steps can be identified with the incoming particle but the walk must ultimately connect with another chain to produce scattering, so that the first large steps are constrained more. For this connection, as Feynman<sup>14</sup> conjectures, the wee region is crucial. It will enter in another way, as we shall see.<sup>15</sup>

The connected walk in the transverse plane can be redrawn as in figure 6. The high multiplicity wee

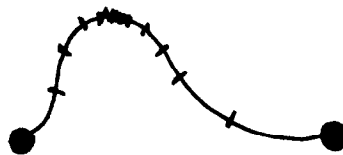


Fig. 6

region on the average of configurations like those in the figure, is a small part of the total scattering area. The density of transverse momentum in this region is high while the density of longitudinal momentum is relatively low. Depending upon the form

taken for the vertices, the whole scattering area may grow with  $s$  due mostly to the increasing size of the first steps. The high multiplicity wee region need not grow but more likely it scales up with  $s$  so that logarithmic or nearly logarithmic multiplicities may obtain.

When the overlap is taken, the contribution of the single ladder to two-particle scattering will have the Regge form if the diffuse large distance regions grow with  $s$ . The large scale fast parton structure is responsible for the exponential behaviour near  $t=0$ , while the small scale central region with its large spatial gradients governs the more slowly falling large  $-t$  behaviour. Note that the coupling constant density in the wee region may play a vital role in determining the rate of growth with energy--an effect found in  $\phi^3$  and to which we shall return.

This attractive picture is complicated by the necessity that fast partons eventually elaborate multiple chains. This will give rise to cuts or absorption. A simple example is shown in figure 7 with some of the eikonal structures which may result when the contribution to two-particle scattering is found. One obtains a sequence of "Regge poles," or a simple Regge-eikonal graph or a Mandelstam cut graph (the

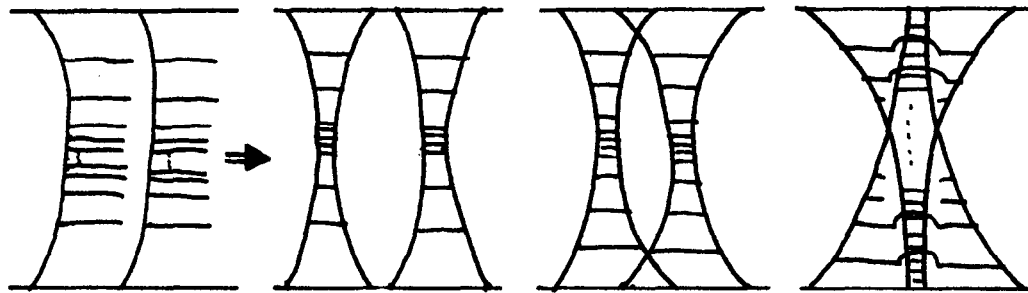


Fig. 7

latter may be seen by isolating a rung at each wide end of a ladder). The AFS cut generated by the Reggeon sequence with the elastic intermediate state is cancelled by the other graphs. Only the Mandelstam cut which is fully nonplanar and has the s-u double spectral function remains. Note that all of these structures result in our construction from the overlap of the diffuse, kinematically "free" large-scale ends of the chains. At small momentum transfers these cuts will probably have the relatively weak effects usually assigned to them.

There is a further possibility, however. This is that the chains themselves may overlap, giving rise to entirely new structures which result not just in absorption but in strong absorption. This possibility is illustrated in fig. 8 . The analogy to the graphs chosen earlier to illustrate the nature of strong absorption is intended.

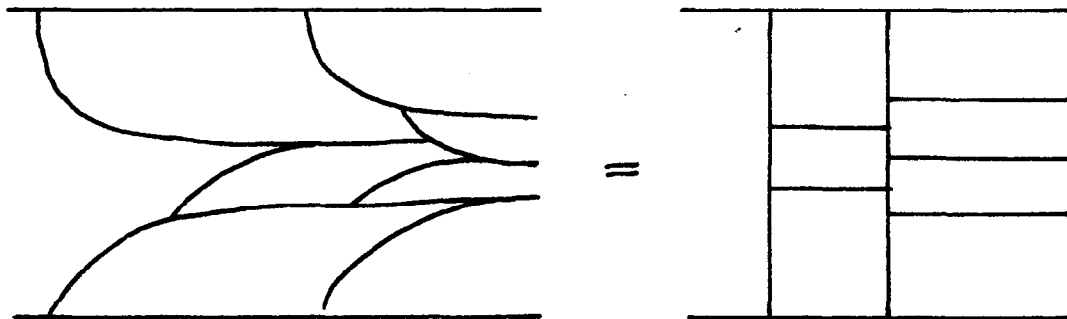


Fig. 8

The most dramatic overlap occurs when a fast or intermediate parton from one chain overtakes the slow dense end of another chain, thus adding a large momentum and removing many wee partons from the central region of the second chain until a new cascade can occur. If, for example, a single multiperipheral chain distributes particles evenly in rapidity, this mechanism will tend to remove particles from the central region and move them into the fragmentation regions.

The possibility that a fast parton may scatter from the dense region of another chain also tends to broaden the transverse momentum distribution of this particle but without appreciably changing its longitudinal momentum distribution, since even in the wee region the density of longitudinal momentum is low. Fast particles in the final state will thus show

broader transverse momentum distributions. The possibility that a fast parton can rescatter, picking up a chain of wees and then cascade decay, may also yield the leading pion effect (Yen and Berger)<sup>16</sup> and produce the low missing mass enhancements observed in many reactions.

All of these effects may be quite small in the total rates since the central region of each chain has small average contribution to the area and the density of fast, long-lived, partons is low. The essential fact however, is that the effects increase at smaller total impact parameter since more overlap configurations are available. This is illustrated in figure 9.

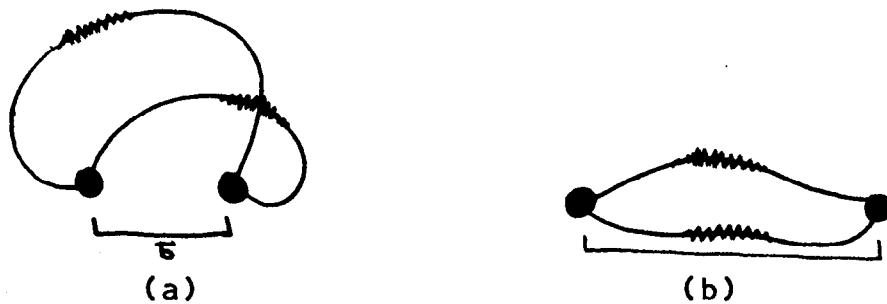


Fig. 9

The parton configurations resulting when all of the possibilities above are taken into account will be very complicated. If the leading partons maintain an identifiable role, then we have available an alternative interpretation. This is the continuum

average or eikonal view. We define the impact parameter as the transverse distance between the centers of mass, suitably defined, of the two clusters. We define the cluster c.m. position by

$$\vec{x}_{cm} = \frac{\sum \eta_i \vec{x}_i}{\sum \eta_i} \quad \sum \eta_i = 1$$

where  $\eta_i$  is the longitudinal fraction associated with the  $i$ th parton at  $\vec{x}_i$ , in analogy with the natural infinite momentum variables. With strong damping of longitudinal momentum transfer, the center of mass of a cluster is very nearly the position of the fastest parton.

Concentrating on these two particles, we can now "cut" all connections to multiperipheral chains, average over configurations and consider the fast partons as propagating in a medium. The density of parton lines seen by each particle determines the scattering. At large impact parameters  $b$  (near the maximum allowed by the energy available to connect the chains), only configurations like those in figure 9.b are involved. The medium seen by each particle is thus diffuse-- the average transverse and longitudinal momentum densities are small--and scattering is small.

At smaller impact parameters, configurations in which fast particles can pass through the dense

central, or small-scale, regions become available. The relative number of such configurations need not be large to have observable consequence. These regions have large transverse momentum densities and low longitudinal momentum densities. Larger values of transverse momentum may thus be transferred to the fast particle and small longitudinal momentum transferred (so that  $t = -\Delta_{\perp}^2$  and the scattering angle is small). The corrections to the eikonal approximation have the form of the spatial gradients  $\partial_{\perp}$  and  $\partial_{\perp}^2$ . With strong damping on longitudinal momenta the gradients  $\partial_{\perp}$  are always small.<sup>17</sup> The transverse derivatives are small here, except at small impact parameters. Note that the first statement would not be true for a point-coupling  $\phi^3$  model since there is no damping on longitudinal momenta down the chain. Two partons prefer to share equally in the incoming longitudinal momentum. One cannot define an eikonal path.<sup>18,19</sup>

The parton construction is susceptible of a fragmentation interpretation in which an incoming right moving parton dissociates into a set of right moving fast partons by cascading. The incoming and outgoing fast partons can then be considered as eikonally scattering in the residual "medium." Each parton has some chance of undergoing larger scattering as before

but the general truth of the fragmentation interpretation rests on the wee regions being small and not causing major rearrangement of the distributions. Otherwise the final state particle might not have resulted from the free dissociation, or cascade, of the incoming particle. Instead it might be part of the "medium" structure associated with the "diffractive" scattering of the incoming particle. This possibility becomes greater as the momentum of the final state particle observed in the diffractively produced cluster becomes lower. These possibilities are illustrated in fig. 10 .

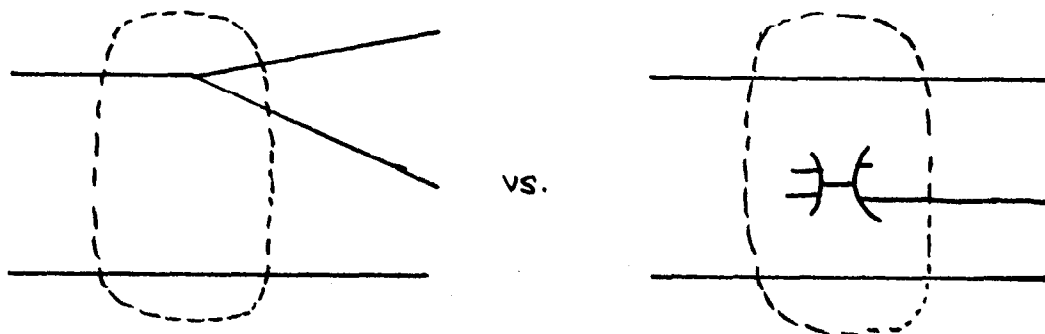


Fig. 10

We can thus establish a relationship between those conditions which give rise to eikonal behaviour of elastic scattering and those configuration space regions which give rise not only to Regge behaviour but also the attending "kinematic" cuts. Both are determined by the large scale 'diffuse' behaviour. The connection is made explicit in the Regge-eikonal model

where exchanged towers are allowed to overlap in all possible ways. The dynamic cuts arising from the small-scale behaviour enter at the level of corrections to the eikonal in elastic scattering and lead to the necessity for strong absorption in inelastic reactions. The parton construction makes clear these connections and indicates that the subtle relation between these two regimes will show up, not only in the transverse spectra but in the longitudinal as well.

#### IV. RE-BORN

Now consider the kinematical properties of our two model Born terms. The simple multiperipheral graph of fig. 1.a may be interpreted as a Feynman diagram, of which our parton model is an example, or as a multi-Regge graph. In the latter case we can also use the parton model description to illustrate its further complexity. Let the produced secondary have momentum  $q$ . We wish to study the relationship between this Born term and the more complicated and shorter range production graph of fig. 3.a. as a function of the magnitude and spatial direction of  $q$ . Let the internal horizontal line of this graph carry momentum  $k$ . In the parton construction of graph "C" suppose  $q$  is in the pionization region and  $k$  is relatively large. As we saw earlier, at smaller impact parameters the fast parton with momentum  $k$  may spatially overlap the following chain. If we represent the vertical exchanges as parton Reggeon chains this overlap will modify the form of the residue, if it occurs, as is likely, in the diffuse large scale region of the second chain. Thus, at larger momentum transfers (smaller initial impact parameter) the presence of the second graph may change the  $t$ -dependence one would need to

ascribe to the upper exchange to make the simple multi-Regge graph alone describe the reaction. As will be seen, this may be equivalent to changing the Regge energy scale,  $s_0$ . There is an analogous effect on the longitudinal spectrum in that the longitudinal momentum of  $k$  may be transferred in part to the produced secondary thus depopulating the multi-Regge region of phase space and producing more fragmentation events. This effect will be relatively small if its possibility rests on the overlap of the fast intermediate parton with the small-scale central region of the second chain. This is one mechanism by which different kinematical regions of production processes may be connected. The resulting correlations, by the above argument, will take the form of only small scale rearrangements of the longitudinal spectrum. As we shall see, the effect on the transverse spectrum will be much more visible if the correct variables are used.

We can also consider the fragmentation region, in which  $q$  has a relatively large longitudinal momentum (with fraction of the incident momentum greater, say, than  $1/\sqrt{s}$ ). In this case one might wish to utilize a wave function and single Regge exchange description of the simple Born term. In the second graph, if  $k$  is large and in the same direction as  $q$  it will overlap

and tend to alter the description of the wavefunction. In particular, it may produce a leading particle effect, low mass enhancements, and resonant structure (see fig. 11). If  $k$  is fast in the other direction it will alter the Regge residue at the lower vertex.

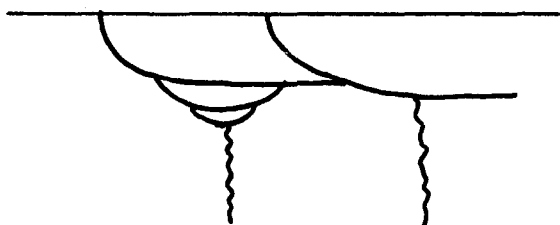


Fig. 11

In this connection, it is interesting to briefly review the logic of Henyey, Kane, Pumplin and Ross<sup>11</sup> in introducing a coherent inelastic" factor multiplying cut terms. The argument was that elastic scattering in the initial or final state of a reaction involving an ordinary inelastic exchange could "diffractively" produce inelastic or resonant intermediate states which had been neglected in constructing cut terms using only elastic unitarity. Representative graphs were of the Mandelstam type. Here we can see not only the origin of this possibility but also the possibility that the Regge structure itself may be altered in even more complex ways. In particular, the presence of a "diffractive"

intermediate state may enhance the production of a similar final state at smaller impact parameters. This region is thus self-enhancing at all impact parameters and is not just peripheral. It favors the low missing-mass region. In the diffractive fragmentation models this vertex structure is put in by hand as  $1/m^2$  or by using  $m^2$  as the Regge energy scale.<sup>20</sup>

In addition to the Born graphs there are graphs in which elastic rescattering, built through eikonal summation of the contributions of the production (and other) graphs to elastic scattering, occurs. By our previous argument, neglect of the shorter range production mechanism results in the necessity for over-absorbing the simple graph. We can now see how this effect may depend (perhaps weakly) upon kinematic region. In what follows we shall usually assume that the longitudinal degrees of freedom are not sufficiently altered by absorption to invalidate the impact parameter representations of subamplitudes and wave-functions used to calculate absorptive effects in the transverse momenta. This is probably a good approximation since it is relatively easy to construct amplitudes which modify longitudinal phase space sufficiently to fit the gross features of production data. We note that multi-Regge models

must be adjusted considerably<sup>21</sup> in the low sub-energy regions to fit the data. From our point of view, the kinematic degrees of freedom opened up by production allow simple tests of these sorts of assumptions within the Regge philosophy.

## V. ABSORPTION AND THE RELATIVISTIC EIKONAL

We now need to consider how to absorb an arbitrary Born term to introduce ordinary absorptive effects. The above discussion will then indicate how to over-absorb to account for other inelastic mechanisms. What is required is a relativistic generalization of the prescriptions of Sopkovich,<sup>22</sup> Gottfried and Jackson,<sup>23</sup> and others.<sup>24</sup> One new feature is retardation, due to which an initial particle is able to act as the source of a field in which a final state particle can eikonally scatter. The kinematic and dynamic conditions under which such rescattering can occur and be described eikonally must also be considered. For example, some particles may have quantum numbers such that they do not couple to the force generating elastic rescattering. Or, if a particle dissociates during inelastic scattering, its fragments may or may not eikonally rescatter in a simple way. From the above discussion, a further desirable condition is that our resulting prescriptions not induce energy dependences which are too strong.

Suppose that elastic scattering is represented by the eikonal summation of all s-channel crossed

ladder graphs involving elementary vector exchange. The resulting amplitude has the form  $isf(t)$  where, with  $\Delta_{\perp}^2 = -t$ ,

$$f(\Delta) = \int d^2b e^{i\Delta \cdot b} \left[ e^{-i\chi_v(\vec{b})} - 1 \right] \quad 5.1$$

The phase is independent of the momenta in the external lines since if we exercise our freedom of path choice for small momentum transfers and choose to expand about the directions  $P \equiv \frac{P_i + P_f}{2}$ ,  $Q = \frac{Q_i + Q_f}{2}$ , then

$$\begin{aligned} \chi_v(\vec{b}) &= \int_{-\infty}^{\infty} d\tau \int_{-\infty}^{\infty} d\sigma P^\mu D_{\mu\nu}(z - 2P\tau + 2Q\sigma) Q^\nu \\ &\cong \frac{P \cdot Q}{4P \cdot Q} \int_{-\infty}^{\infty} dz_0 \int_{-\infty}^{\infty} dz_3 \Delta_F(z) \\ &\approx -iK_0(mb) \end{aligned} \quad 5.2$$

The (explicitly unitary) elastic S-matrix in b-space

$$S_{el} = e^{-i\chi_v(\vec{b})} \quad 5.3$$

then goes to one for large  $b$  and vanishes for  $b$  near zero. The corresponding T-matrix is central in b-space, pure imaginary, and does not change with energy (no shrinkage). All of this corresponds to the exchange of a real  $j=1$  fixed pole in the t-channel. <sup>25</sup> We would clearly not want to exchange this object more

than once. The vector exchange, which is used to represent all the exchanges contributing to elastic scattering, keeps track of the correct counting.

The above analysis can be extended to the case of two particles interacting through the exchanges represented by the fields A and C. For example, A might be the pion field and C the vector field of the previous example. In the external field approximation, the T-matrix for particle 1 scattering in the field  $V(x) = C(x) + aA(x)$  may be written as a local functional  $T\langle V \rangle = T\langle C(x) + aA(x) \rangle$ . If C and A commute, in the sense that the particle couples in the same way to C independently of the number of interactions with A, then we can use the usual functional methods to calculate the two-particle T-matrix.<sup>26</sup> The analogue of the Levy-Sucher form for this quantity<sup>27</sup> is

$$T_{12} \propto i \int_0^1 d\lambda \int d^4z e^{2i\vec{\Delta}_i \cdot \vec{z}_L} \left[ g^2 D_C(z) + a^2 g'^2 D_A(z) \right] e^{-i\lambda(\chi_C + \chi_A)} \quad 5.4$$

where  $g$  and  $g'$  are the couplings of the external particles to fields C and A, and the eikonal phase integrals are

$$\chi_c = g^2 \iint_0^\infty d\tau d\sigma \left\{ D_c(z + 2P_1\tau - 2Q_1\sigma) + D_c(z - 2P_1\tau - 2Q_1\sigma) \right. \\ \left. + D_c(z + 2P_1\tau + 2Q_1\sigma) + D_c(z - 2P_1\tau + 2Q_1\sigma) \right\}$$

$$\chi_A = \chi_c (g^2 \rightarrow a^2 g'^2, c \rightarrow A) \quad 5.5$$

This represents the sum of all crossed s-channel ladders whose rungs are the quanta of A and C. If C represents vector exchange then  $\chi_c$  will be independent of s while if A represents spin  $J < 1$   $\chi_A$  will fall with s and the Born term of A will tend to dominate the high energy behaviour. Under certain conditions the expression for  $T_{12}$  will simplify. Pick the momentum transfer,  $2\Delta$ , purely transverse and do the integral over  $\lambda$ . Now, if the eikonal path can be defined as along the average of initial and final momenta as before, then

$$\chi_c \rightarrow g^2 \iint_{-\infty}^\infty d\tau d\sigma D_c(z - 2P_1\tau + 2Q_1\sigma) \quad 5.6$$

and similarly for  $\chi_A$ . This choice of path makes the eikonal phase independent of  $z_+$  and  $z_-$ . All integrals then decouple except those over transverse variables. In particular, the numerator and denominator factors cancel, leaving a simple expression for  $T_{12}$ :

$$T_{12} \propto - \int d^2b e^{-2i\vec{\Delta} \cdot \vec{b}} \left\{ e^{-i(\chi_A + \chi_C)} - 1 \right\} \quad 5.7$$

Projecting the lowest order contribution to the inelastic final state, single A exchange,

$$T_{if} \propto i \int d^2b e^{-2i\vec{\Delta} \cdot \vec{b}} \chi_A e^{-i\chi_C} \equiv i \int d^2b e^{-2i\vec{\Delta} \cdot \vec{b}} \chi_A(b) S_C(b) \quad 5.8$$

This is the result one would expect. It rests on the commutivity of the interactions and upon the simplification resulting from the particular identification of an eikonal path. The direction  $P = P_i + P_f$  for example, can be expected to give approximately the same phase integral as the sum of phase integrals for interactions crossing the inelastic exchange in all possible ways if  $P_i \cong P_f$ . This is just the condition that the initial and final states have the same impact parameter representation. <sup>28</sup> Another way of saying this is that the exchanges are uncorrelated in impact parameter space. It is possible to be more careful and produce other expressions but to leading order in the eikonal expansion all are nearly equivalent. The differences usually occur at the same level as the first order corrections that is, down by  $\Delta\sqrt{s}$ .

If the elastic and inelastic exchanges fail to commute, as would be the case for example in with an elastic interaction which couples only to charge, then simplification depends upon other factors. Suppose particle one enters an interaction in a state which couples elastically to a field I, changes state through an inelastic exchange of type A, and exits in a state which couples elastically to F. Let particle two couple to I', A, and F' in the same sequential way. Note that if I=I' and F=F' with I≠F, the inelastic exchange will separate initial and final state interactions as in the non-relativistic case.

With the same choice of eikonal path as before, the two-particle T-matrix, to lowest order in the inelastic exchange, is

$$T_{12} = \int d^4z e^{i\vec{\Delta}_1 \cdot \vec{z}_1} D_A(z) e^{-i[\chi_{II'} + \chi_{FF'} + \chi_{IF'} + \chi_{FI'}]} \quad 5.9$$

where we have chosen a center of mass frame where the momentum transfer is purely transverse and

$$\chi_{II'}(z) = \int_{-\infty}^0 d\tau \int_{-\infty}^0 d\sigma D_{II'}(z + 2P\tau - 2Q\sigma)$$

$$\chi_{IF'}(z) = \int_{-\infty}^0 d\tau \int_0^{\infty} d\sigma D_{IF'}(z + 2P\tau - 2Q\sigma)$$

$$\begin{aligned} \chi_{FI'}(z) &= \int_0^\infty d\tau \int_{-\infty}^0 d\sigma D_{FI'}(z + 2P\tau - 2Q\sigma) \\ \chi_{FF'}(z) &= \int_0^\infty d\tau \int_0^\infty d\sigma D_{FF'}(z + 2P\tau - 2Q\sigma) \end{aligned} \quad 5.10$$

The D's represent propagation of the appropriate exchanges, including the couplings to the external lines.

The integrals over longitudinal variables in this expression are still coupled. Suppose the inelastic exchange has relatively short range in  $z_+$  and  $z_-$ . If the phase integrals receive small contribution from this region or if the contribution of each of the four phase integrals over the region is approximately the same, then one can set  $z_+ \cong 0$  and  $z_- \cong 0$  in the phase integrals with only small error. The integration over the longitudinal variables of the inelastic exchange may then be done independently, resulting in an impact parameter representation. If, in addition, the phase integrals are invariant under  $z_+ \rightarrow -z_+$ ,  $z_- \rightarrow -z_-$ , we can identify the relativistic version of the familiar Sopkovich prescription:

$$T_{12} = \int d^2b e^{i\Delta \cdot b} \chi_A(b) [S_{II'}, S_{FF'}, S_{IF'}, S_{FI'}] \quad 5.11$$

where

$$S_{ij} = e^{-i\chi_{ij}}, \quad \chi_{ij} = \int_{-\infty}^{\infty} dt \int d\sigma D_{ij}(z - 2P\tau + 2Q\sigma) \quad 5.12$$

We should note that this symmetry will not in general be a property of the exchange mechanisms. If it is, this implies that in reactions where only one factor  $S_{ij}$  is different from one (e.g.,  $e^+e^- \rightarrow \bar{h}h$ ), absorptive effects may be different from the Sopkovich prescription,  $S^{1/2}$ .

It is easy to see how the nonrelativistic potentials, which involve only the relative coordinate  $z$ , are related to the phase integrals above. Consider  $\chi_{II'}$  above. In the center of mass where, say,  $P=(E, 0, P)$ ,  $Q=(E, 0, -P)$ , we can rescale and change variables:

$$\chi_{II'} = \frac{1}{8EP} \int_{-\infty}^{\infty} dt \int_{-\infty}^z d\vec{z} D_{II'}(t, \vec{z}, \vec{b}_\perp) \quad 5.13$$

so if we define the "potential"

$$U_{\text{initial}}(\vec{z}, \vec{b}) \equiv \frac{1}{4EP} \int_{-\infty}^{\infty} dt D_{II'}(t, \vec{z}, \vec{b}_\perp) \quad 5.14$$

the connection is clear.

All of the preceding discussion can be generalized to the exchange of more complicated objects. In particular, the inelastic exchange may be

a multi-Regge chain. This will be consistent with the eikonal treatment if there are still identifiable leading particles which allow definition of an eikonal path. The energy independence of the vector exchange model for elastic rescattering makes the energy loss to the secondaries less relevant than otherwise, as long as it is not too great.

In the treatment of particular exclusive production channels it will usually be assumed that the exchanges which contribute to rescattering couple in the same way to all hadrons. Since we would also like to exploit our knowledge of two-particle reactions in building multiparticle amplitudes, we will usually assume that all absorptive effects between the particles involved in two-body subamplitudes are incorporated in those subamplitudes. The parton model discussion indicates that absorptive effects, for example, between even next-to-nearest neighbors on a multi-Regge chain may be incorporated in the vertex structures (residues). Hence the dominant, experimentally accessible effects will be those due to absorption between particles widely separated in longitudinal momentum. We now proceed to a more detailed discussion of these effects.

The subamplitudes utilized to construct

multiparticle amplitudes will be written in the conventional impact parameter representation, where the radii involved may be dependent upon the particular subenergy. Spin coupling factors can be deduced from the correspondence between the rotation functions, in a helicity basis, and the appropriate Bessel functions<sup>29</sup>:

$$d_{\lambda, \mu}^j(z_s) \xrightarrow[\substack{j \rightarrow \infty \\ z_s \rightarrow 1}]{\quad} J_{|\lambda - \mu|}(b\sqrt{t}) \quad 5.15$$

where  $\lambda$  is the helicity difference in the initial state,  $\mu$  that in the final state ( $\lambda = \lambda_a - \lambda_b$ ,  $\mu = \lambda_c - \lambda_d$ ). The general amplitude for helicity flip  $\Delta\lambda = |\lambda - \mu|$  will then be written in the form

$$f_{\Delta\lambda}(s, t) \underset{t \approx -\Delta_\perp^2}{=} i\pi s \int db \, b f_{\Delta\lambda}(s, b) J_{\Delta\lambda}(b\Delta) \quad 5.16$$

We would like to rewrite this in Fourier transform form. For  $\Delta\lambda=0$ , the result is trivial:

$$f_0(s, \Delta) = \frac{i s}{2} \int d^2b \, e^{i\vec{b} \cdot \vec{\Delta}} f_0(b, s) \quad 5.17$$

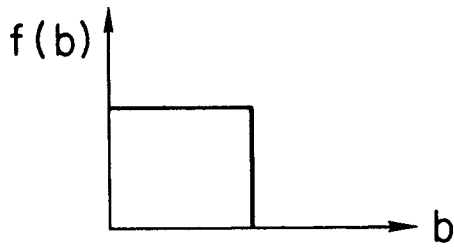
For  $\Delta\lambda=1$ , noting that  $J_1(z) = -(d/dz)J_0(z)$  allows us to write

$$f_1(s,t) = \frac{-iS}{2} \frac{d}{d\Delta} \left[ \int d^2b e^{i\vec{b}\cdot\vec{\Delta}} \frac{f_1(s,b)}{b} \right] \quad 5.18$$

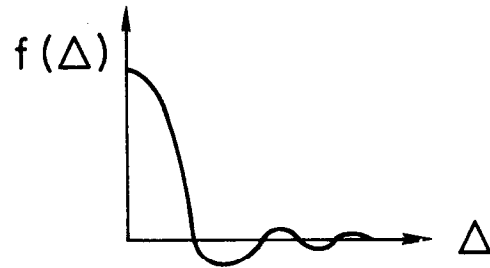
The spin coupling is thus sensitive to the direction of  $\vec{b}$  as one would expect. This form will be particularly useful in multiparticle amplitudes. If the absorptive factor is azimuthally symmetric then it will not alter this spin structure (it may not be azimuthally symmetric). In multiparticle amplitudes however, overall absorption (that is in the total impact parameter) will alter the effective spin coupling by preferring special directions of the sub-amplitude impact parameter. Higher order couplings may be written down from the Fourier representation of  $J_n$ .

Different impact parameter distributions give very different  $t$ -distributions. A few possibilities, all of which give a forward peak in  $t$ , are shown in fig. 12. The radii may be energy dependent without loss of generality. Most model amplitudes considered below will be constructed from Gaussian subamplitudes for calculational convenience and since they are devoid of  $t$ -structure. More precise forms will be used to make comparison with particular reactions. The elastic rescattering will always utilize a Gaussian T-matrix, except for a brief qualitative discussion of the

Black Disc:

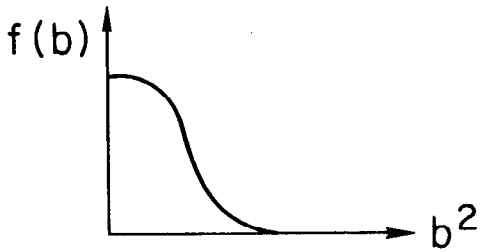


$$f(b) = \theta(R-b)$$

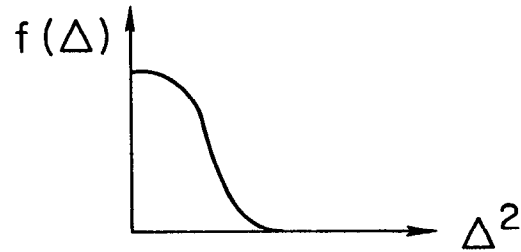


$$f(\Delta) = \frac{R}{\Delta} J_1(R\Delta)$$

Im (Pomeron):

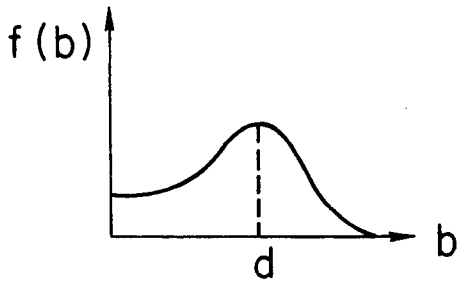


$$f(b) = e^{-b^2/2R^2}$$



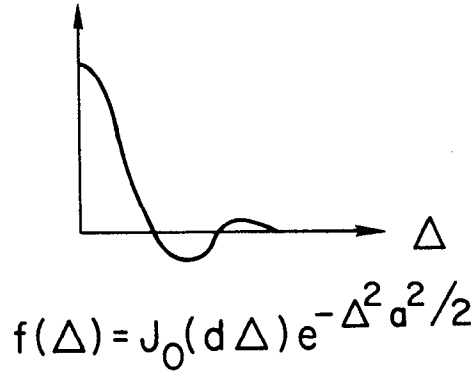
$$f(\Delta) = e^{-\Delta^2 R^2/2}$$

Peripheral:



$$f(b) = \int d\Omega_d e^{-\frac{(\vec{b}-\vec{d})^2}{2a^2}}$$

$$= e^{-\frac{(b^2+d^2)}{2a^2}} I_0\left(\frac{bd}{a^2}\right)$$



$$f(\Delta) = J_0(d\Delta) e^{-\Delta^2 a^2/2}$$

215082

Fig. 12

alternative forms for the real part of the elastic amplitude which is present at finite energies. The presence and location of zeros in  $t$ -distributions depends very sensitively upon the precise shape of the impact parameter amplitude.<sup>30</sup> Also, since our primary interest is in qualitative features and relative normalizations, absolute normalizations will be consistently ignored.

In constructing phenomenological absorbed two-particle amplitudes it is often found that real and imaginary parts of the input exchange must be absorbed with different strengths in order to fit experiment. Differences between helicity flip and non-flip amplitudes arise and polarization studies directly reflect this difficulty. The success of strong or weak cuts depends upon where they are applied.<sup>31</sup>

Experimental studies show, for example, that in  $\pi N$  scattering the imaginary part of the isovector exchange (probably  $\rho$ ) non-flip amplitude requires strong absorption while the real part is weakly absorbed. There are of course many ways in which this could happen. The most obvious is that the complex  $t$ -dependent Regge phase in the Born term already includes absorption.<sup>32</sup> It is difficult to make a systematic statement of this possibility, however. A more attractive reason is that the absorption is

complex, corresponding to a real part in the elastic amplitude at machine energies. In our parametrization, with  $S(b)=1-iT(b)$  and  $T(b)=iT(b)$ ,  $\lambda$  may be complex at finite energies with, say, an imaginary part about 30% that of the real. If we write  $\lambda = \alpha + i\beta$  and take an input Born amplitude with equal real and imaginary parts (e.g., rho-exchange at  $t=0$ ),  $\text{Amp}=A(b)\cdot(1+i)$ , then the output amplitude has the form

$$\text{Amp} = A(b) \cdot \left[ (1 - (\alpha - \beta)\tau(b)) + i (1 - (\alpha + \beta)\tau(b)) \right]$$

That is, the imaginary part is much more strongly absorbed than the real part if  $\beta > 0$ . Consistent with our bound on  $|\lambda|$ , we may take  $\alpha = 1.5$  and  $\beta = 0.5$  so that the real part is absorbed with strength 1.0, the imaginary with strength 2.0, satisfying weak and strong cut prescriptions in the right places. One might expect the imaginary part of  $\lambda$  to depend upon  $b$  and  $s$ , perhaps vanishing as  $s \rightarrow \infty$ . Absorptive cuts also tend to induce dips in  $t$ -distributions. An imaginary part will tend to fill these dips. These and other effects will also appear in the absorbed multiparticle amplitudes, to which we now turn.

## VI. CONSTRUCTION OF MODELS

As a first model, consider the absorbed multi-peripheral model for the production of  $N$  secondaries of fig. 13a (page 62). A complete set of variables is the set of  $N+1$  subenergies and the  $N+1$  two-dimensional vectors  $\vec{b}_i$  (which is equivalent to  $N+1$  lengths and  $N$  angles, where the latter are analogous to the angles in Toller analysis)<sup>33</sup>. This decomposition is invariant under boosts normal to the transverse plane. The corresponding amplitude is

$$M_{2 \rightarrow N+2} \propto \int d^2B S(B) \prod_{j=1}^{N+1} \left[ \int d^2b_j e^{i\vec{b}_j \cdot \vec{k}_j} T_j(b_j, s_j) \right] \delta^{(2)}(\vec{B} - \sum b_i) \quad 6.1$$

where  $\vec{k}_j$  is the transverse momentum along  $\vec{b}_j$ ,  $T_j$  is the two-particle subamplitude corresponding to momentum transfer  $k_j$  and subenergy  $s_j$ . Other functions  $f(b_i, b_j)$  can be introduced, for example, to account for non-nearest-neighbor absorptive effects. As we argued before, however, if realistic parametrizations of the  $T_j$  are used, some of these effects are already included. Note that if  $S(B)=\text{constant}$ , so that there is no rescattering, the integrals over  $b_j$  decouple and the usual random walk in transverse configuration space occurs since the direction of each spatial vector  $\vec{b}_j$  is

then unconstrained. The effect of non-trivial  $S(B)$  is to constrain the beginning and end of the walk, and hence the direction of each intermediate step. Other absorptive effects would constrain internal points.

The absorptive factor is chosen as

$$S(B) = 1 - \lambda e^{-B^2/2R^2(s)} \quad 6.2$$

This corresponds to a purely absorptive elastic scattering amplitude normalized as

$$T(s, B) = 4\pi i s e^{-B^2/2R^2} \quad 6.3$$

or

$$\begin{aligned} T(s, t) &= \int \frac{d^2B}{2\pi} e^{-i\vec{B} \cdot \vec{\Delta}} T(s, B) \\ &= i s (4\pi R^2) e^{\frac{R^2}{2} t} \end{aligned} \quad 6.4$$

so that

$$\sigma_{\text{Tot}} = \frac{1}{s} \text{Im } T(s, 0) = 4\pi R^2$$

$$\sigma_{\text{el}} = \pi R^2 \quad 6.5$$

$$\frac{d\sigma_{\text{el}}}{dt} = \pi R^4 e^{R^2 t}$$

The two-particle subamplitudes are written as

$$T_i(s_i, b_i) = \frac{f(s_i)}{R_i^2} e^{-\vec{b}_i^2/2R_i^2(s_i)} \quad 6.6$$

or

$$T_i(s_i, \Delta_i) = f(s_i) e^{-\frac{R_i^2}{2} \Delta_{i\perp}^2} \quad 6.7$$

The normalization  $1/R_i^2$  is chosen so that each random walk step has unit probability, independent of the associated radius--that is

$$\int \frac{d^2 b}{2\pi} \frac{e^{-b^2/2R^2}}{R^2} = 1 \quad 6.8$$

The step probability is then just the coefficient function of  $s_i$ . Regge behaviour, with linear trajectories, would imply

$$\begin{aligned} \frac{R_i^2}{2} &\approx a_i + \alpha_i' \ln \frac{s_i}{s_0} \\ f(s_i) &\approx \left(\frac{s_i}{s_0}\right)^{\alpha_{i0}} \end{aligned} \quad 6.9$$

apart from (t-dependent) signature factors.

Rewriting Equation 6.1, with the delta-function in parametric form and dropping explicit reference to the energy dependences, one has

$$M_N = \int \frac{d^2 \gamma}{(2\pi)^2} \int d^2 B S'(B) e^{i\vec{B} \cdot \vec{\gamma}} \prod_{i=1}^{N+1} T_i(\vec{k}_i - \vec{\gamma}) \quad 6.10$$

where

$$\begin{aligned} T_i(\vec{\delta}_i) &= \int \frac{d^2 b_i}{2\pi} e^{i\vec{b}_i \cdot \vec{\delta}_i} T_i(b_i) \\ &= e^{-\frac{R_i^2}{2} \delta_i^2} \end{aligned} \quad 6.11$$

With the above choice of  $S(B)$  the integral over  $B$  can be done

$$\begin{aligned}
S(\vec{\tau}) &= \int \frac{d^2 B}{2\pi} e^{i\vec{B} \cdot \vec{\tau}} [1 - \lambda e^{-B^2/2R^2}] \\
&= 2\pi \delta^{(2)}(\vec{\tau}) - \lambda R^2 e^{-\frac{R^2}{2} \tau^2}
\end{aligned} \tag{6.12}$$

Then the integral over  $\vec{\tau}$  itself gives

$$M_N = e^{-\frac{1}{2} \sum_{i=1}^{N+1} R_i^2 K_i^2} \left[ 1 - \frac{\lambda R^2}{\rho} e^{+\alpha^2/2\rho} \right] \tag{6.13}$$

where

$$\begin{aligned}
\vec{\alpha} &\equiv \sum_{i=1}^{N+1} R_i^2 \vec{K}_i \\
\rho &\equiv R^2 + \sum_{i=1}^{N+1} R_i^2
\end{aligned} \tag{6.14}$$

All of these quantities are quite simple in the Regge parametrization when all subamplitudes have  $a_i = 0$  and a common slope of one, so that  $R_i^2 \approx \ln s_i$  and

$$\begin{aligned}
\vec{\alpha} &= \sum_{i=1}^{N+1} (\ln s_i) \cdot \vec{K}_i \\
\rho &\approx 2 \ln s
\end{aligned} \tag{6.15}$$

Taking  $R^2 \approx \ln s$  and noting that in the multi-Regge region  $\sum \ln s_i \approx \ln s$ , the amplitude becomes

the amplitude becomes

$$M_N^{\text{M.R.}} \propto e^{-\frac{1}{2} \sum \ln s_i K_i^2} \left\{ 1 - \frac{\lambda}{2} e^{\frac{(\sum \ln s_i R_i)^2}{2 \ln s}} \right\} \tag{6.16}$$

If in addition  $\ln s_i = (\ln s)/(N+1)$  and  $\langle N+1 \rangle = \ln s$ ,

$$M_N^{M.R.} \propto s^{\alpha_0} e^{-\frac{\ln s}{2} \sum_i^{N+1} \vec{k}_i^2} \cdot \left\{ 1 - \frac{\lambda}{2} e^{(\sum \vec{k}_i)^2 / 2 \ln s} \right\} \quad 6.17$$

The multi-regge contribution is thus damped by absorption with the largest damping when the momentum transfers  $\vec{k}_i$  are aligned. The optimal variable for observing this effect is thus  $\sum_i \vec{k}_i$ . The contribution to elastic scattering can be calculated. If  $\alpha_0 = 1.0$ ,  $\sigma$  violates the Froissart bound unless the absorption parameter has the value  $\lambda = 2.0$ , in which case the contribution of the multi-Regge region vanishes asymptotically. Note that the problem arises when the chain is straight and of small length  $B$  (which is conjugate to the large vector  $\sum \vec{k}_i$ ), so that the production is dense in configuration space.<sup>1</sup> Absorption damps the effect of this region as we saw in the general parton discussion, redistributing the production into non-multi-Regge regions. In this connection note that the absorptive factor in the amplitude is a power series in  $1/\ln s$ .

Returning to the general case of Equation <sup>6.13</sup>  $A$ , the distribution  $d\sigma/d\alpha^2$  is easily calculated. Defining

$$A(\alpha) \equiv 1 - \frac{\lambda R^2}{\rho} e^{\alpha^2 / 2\rho} \quad 6.18$$

squaring the amplitude, and introducing

$$\delta^{(1)}(\vec{\alpha} - \sum_i R_i^2 \vec{k}_i) = \int \frac{d^2x}{(2\pi)^2} e^{i\vec{x} \cdot (\vec{\alpha} - \sum R_i^2 \vec{k}_i)} \quad 6.19$$

one has

$$\frac{d\sigma^{(N)}}{d\alpha^2} = \left[ \int f(s_i) d\rho_N(s_i) \right] \cdot e^{-\frac{\alpha^2}{\sum R_i^2}} \cdot A^2(\alpha) \quad 6.20$$

where  $d\rho_N(s_i)$  is the residual phase space, and where it has been assumed that the damping in the transverse momenta is sufficient to allow one to perform these integrations independently of energy conservation. Monte Carlo calculations with exact phase space, presented below, show this to be a very good approximation at high energy. If one assumes (nearly) energy independent radii, with  $R_i^2 = r^2$ , then the rest of the phase space integrals may be done. With  $\vec{v} = \vec{\alpha}/r^2 = \sum_i \vec{k}_i$ , the result is

$$\frac{d\sigma^{(N)}}{dv^2} \propto e^{-\frac{r^2 v^2}{N+1}} \cdot \left[ 1 - \frac{\lambda}{1+\beta} e^{+\frac{\beta r^2 v^2}{2(1+\beta)(N+1)}} \right]^2 \quad 6.21$$

where  $\beta = (N+1)r^2/R^2$

The large  $v^2$  region is greatly modified by

absorption with more events in this kinematic region than if  $\lambda = 0$ . This vector is easily rewritten in terms of final state momenta, labeled according to fig. 13a, as

$$\vec{v} = \sum_{j=1}^{N+1} \vec{k}_j = \left(\frac{N+1}{2}\right)(\vec{k} - \vec{n}) + \sum_{j=1}^N \vec{p}_j \cdot \left(\frac{N+1}{2} - j\right) \quad 6.22$$

Note that if, as in the M-R. case,  $\beta = 1$ , the overall slope of the distribution is a function of  $R^2/(N+1)$  ( $\cong 1/\ln s$ ) and hence decreases with increasing multiplicity. The slope in the absorptive factor behaves in the same fashion but is smaller by a factor of  $1/4$ . Larger values of  $v^2$  will be found at higher energies. Calculation shows that the transverse momentum distributions, single and relative, of the secondaries are not significantly broadened by the absorption.

The variable  $v^2$  is theoretically optimal but experimentally somewhat inaccessible, particularly for higher multiplicities. It is therefore of interest to determine the effects upon other distributions. One proceeds, as above by introducing delta-functions in parametric form to free the phase space integrations. The distribution in the relative transverse momentum of the leading outgoing particles,  $\vec{w} = \vec{k} - \vec{n} = \vec{k}_1 + \vec{k}_{N+1}$ , is

particularly convenient for experimental analysis. For  $N=1$ , the variables  $w$  and  $v$  are identical. We give the results in two cases. The first corresponds to the M-R. case in which the subamplitude radii are smaller than the overall radius-- that is  $r^2 = R^2/(N+1)$ . The other is characteristic of a purely geometric model with fixed radii and  $r^2 = R^2$ .

Again ignoring the phase space constraints, the distributions in the relative transverse momentum of the leading particles,  $\vec{w}$ , are

$$\frac{d^2\sigma}{dw^2} \underset{r^2=R^2}{=} e^{-\frac{R^2}{2}w^2} \left[ 1 - \frac{4\lambda}{N+5} e^{\frac{R^2 w^2}{N+5}} + \frac{\lambda^2}{3(N+2)} e^{\frac{R^2 w^2}{3}} \right]$$

$$\frac{d^2\sigma}{dw^2} \underset{r^2=R^2/(N+1)}{=} e^{-\frac{R^2 w^2}{2(N+1)}} \left[ 1 - \frac{4\lambda}{3N+5} e^{\frac{R^2 w^2}{(3N+5)(N+1)}} + \frac{\lambda^2(N+1)}{2(N+3)} e^{\frac{R^2 w^2}{(N+1)(N+3)}} \right] \quad 6.23$$

For  $N=1$ , the variables  $w$  and  $v$  are identical. The effect of absorption on these distributions is striking. The general effect is to steepen the forward ( $w^2$  near zero) peak (and the  $v^2$ ) and broaden the large  $w^2$  (and  $v^2$ ) region. The transverse momentum distribution of a single leading particle has the form

$$\frac{d^2\sigma}{dk^2} \Big|_{r^2=R^2} = e^{-R^2 k^2} \left[ 1 - \frac{4\lambda}{N+4} e^{\frac{R^2 k^2}{N+4}} + \frac{\lambda^2}{2(N+2)} e^{\frac{R^2 k^2}{2}} \right]$$

$$\frac{d^2\sigma}{dk^2} \Big|_{r^2=R^2/(N+1)} = e^{-\frac{R^2 k^2}{N+1}} \left[ 1 - \frac{4\lambda(N+1)}{3N+4} e^{\frac{R^2 k^2}{(N+1)(3N+4)}} + \frac{\lambda^2(N+1)}{2(N+2)} e^{\frac{R^2 k^2}{(N+1)(N+2)}} \right] \quad 6.24$$

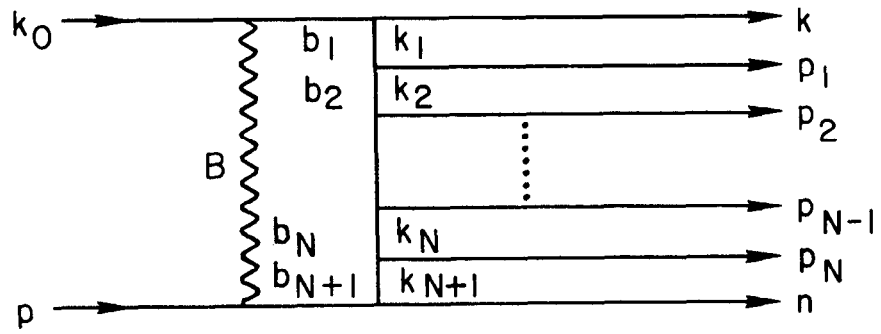
Both of these distributions are consistent with the experimental observation that the transverse momentum distributions, dominated by the first factor above, do not change appreciably with energy. In the case  $r^2 = R^2$  one expects  $R^2 = \text{constant}$ , while if  $r^2 = R^2/(N+1)$  then one expects  $R^2 \approx \langle N+1 \rangle \approx \ln s$ . In both cases, the small transverse momentum regions do not change with  $s$ . The absorption distinguishes between these possibilities however--the last expression yields more large transverse momentum events as  $s$  increases. The latter will also be a characteristic of the polyperipheral model to be introduced below (and which will have equal radii). It is also interesting that leading particles will display broader transverse momentum distributions than the secondaries.

The broadening of the transverse momentum distributions is not the only effect. The leading particle distributions should display breaks or shoulders at moderate values of  $P_{\perp}^2$ . In the reaction

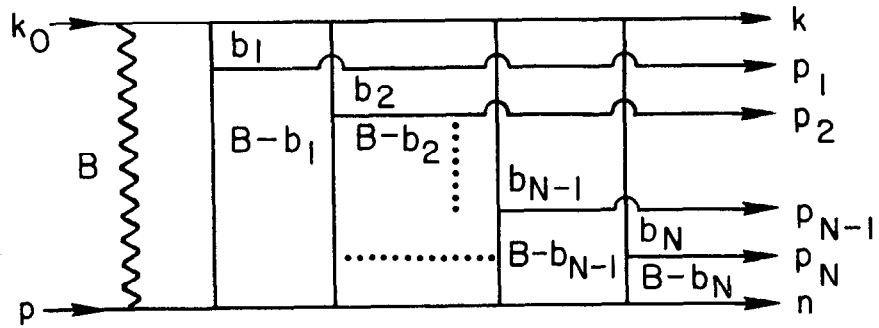
described below this will come at about  $P_{\perp}^2=0.25$ . The secondaries will not show this structure since they have been rescattered with great frequency and in random directions before emerging.

A particularly clean experiment with which to compare is the reaction  $\pi^-P \rightarrow \pi^- \pi^+ \eta$ .<sup>34</sup> The longitudinal distributions, shown in fig. 14, allow almost no ambiguity in discriminating leading particles. There is little  $\rho$ -contribution. The experimental distributions in  $v^2$ , the relative momentum between a pair of adjacent particles, and the individual particle transverse momenta, for incident pion energy of 16 GeV, are shown in figure 15.

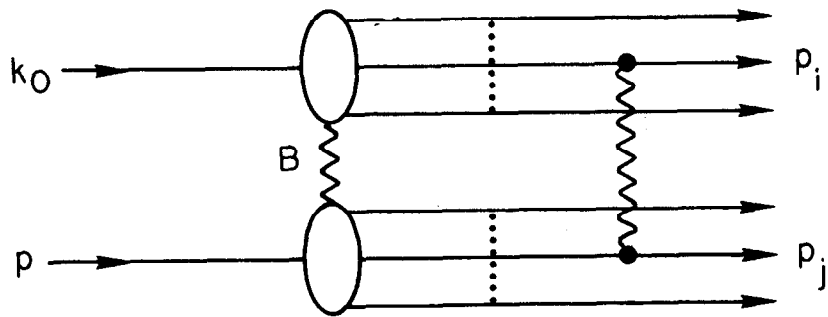
In fig. 16 we present the theoretical predictions for various absorption strengths. The curves were produced by Monte Carlo event generation, weighted by the amplitude of eqn. 6.13 with common radius  $R^2=8.0$ . This avoids any neglect of energy conservation that our analytic expressions might involve. Comparison indicated that the approximations in the latter are quite accurate. The results of the Monte Carlo generation were fed into an analysis routine which produced nearly all possible longitudinal and angular distributions. In order to fit the corresponding experimental longitudinal distributions



(a)



(b)



(c)

2005A4

Fig. 13

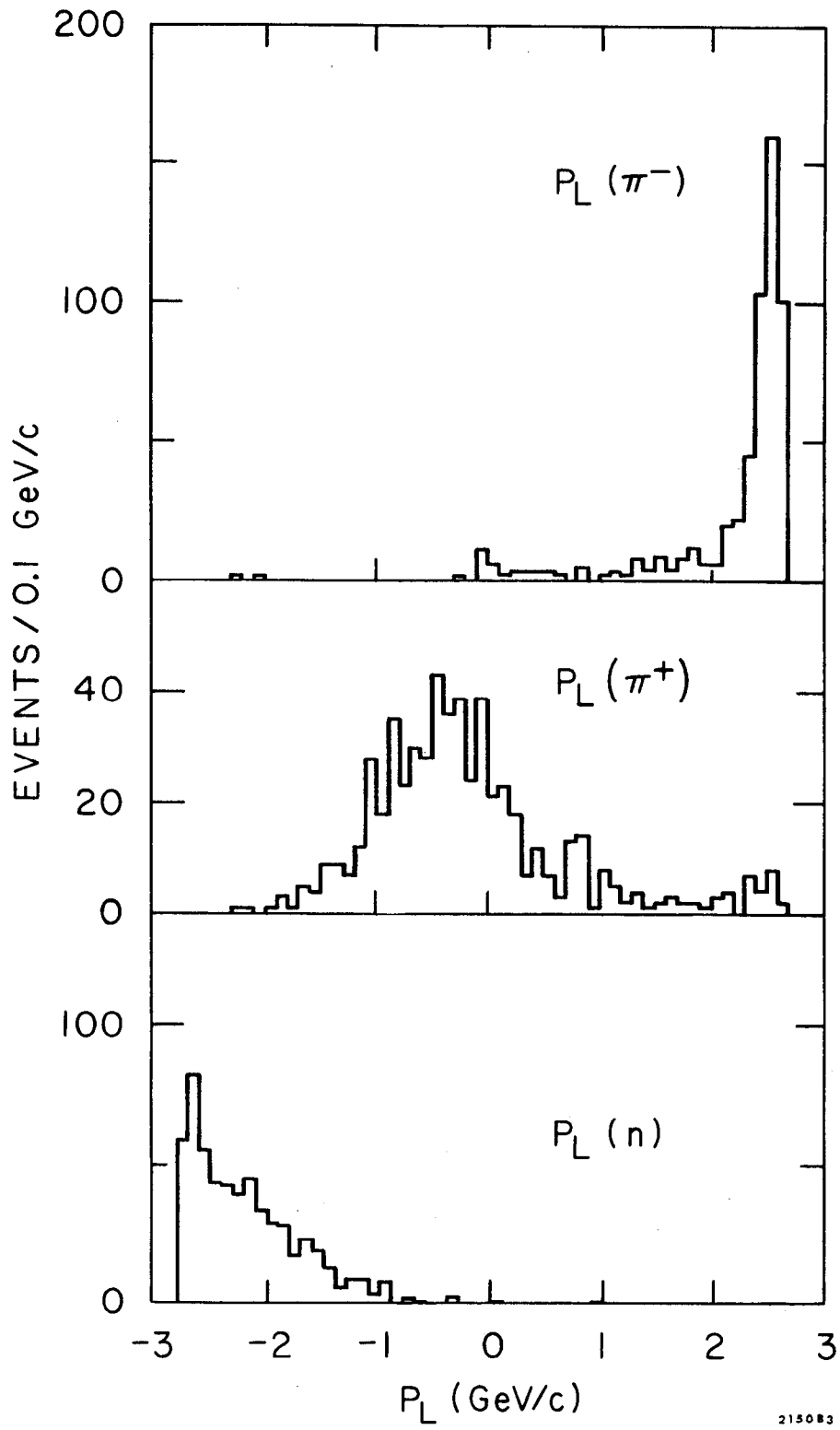
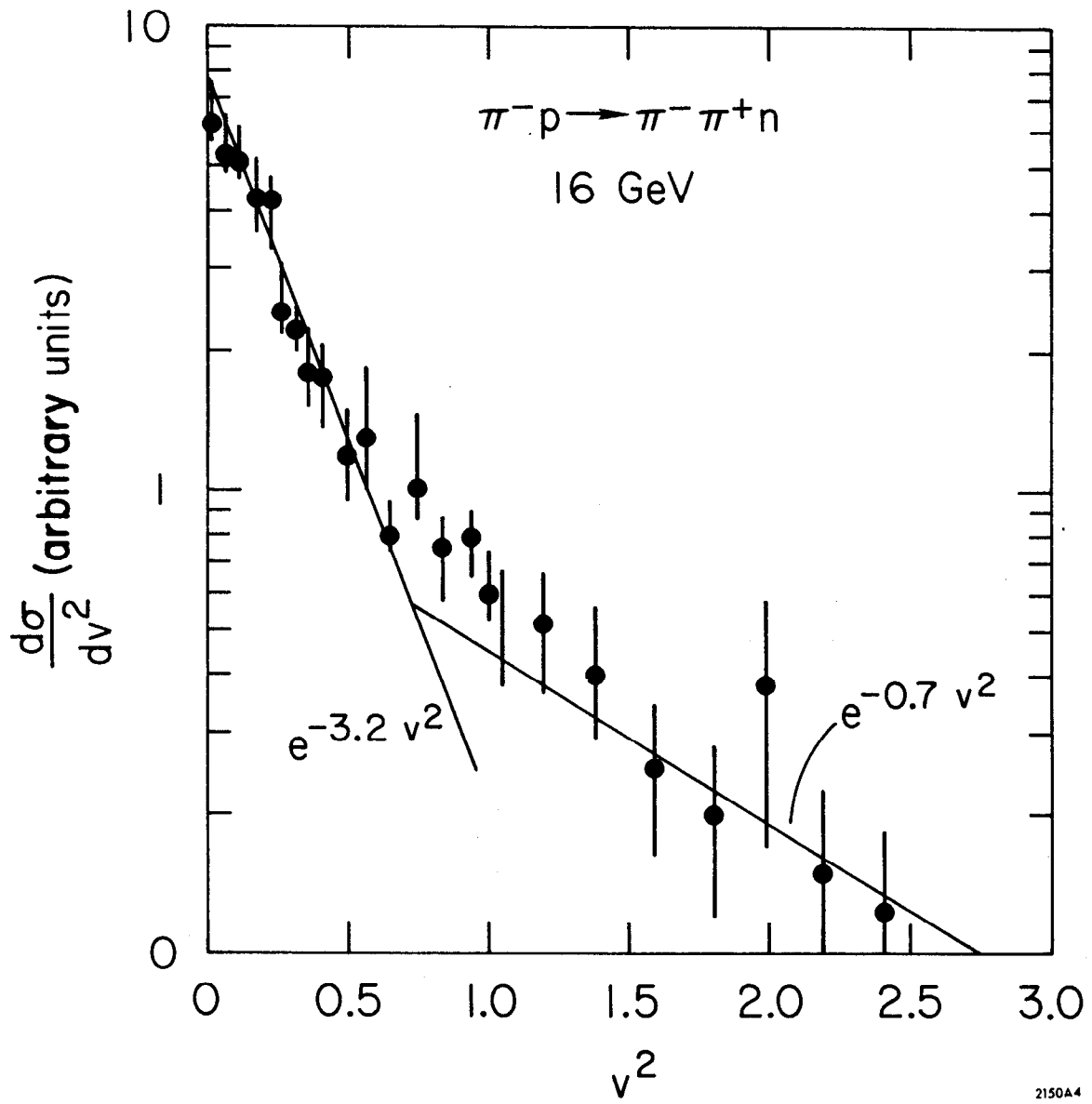
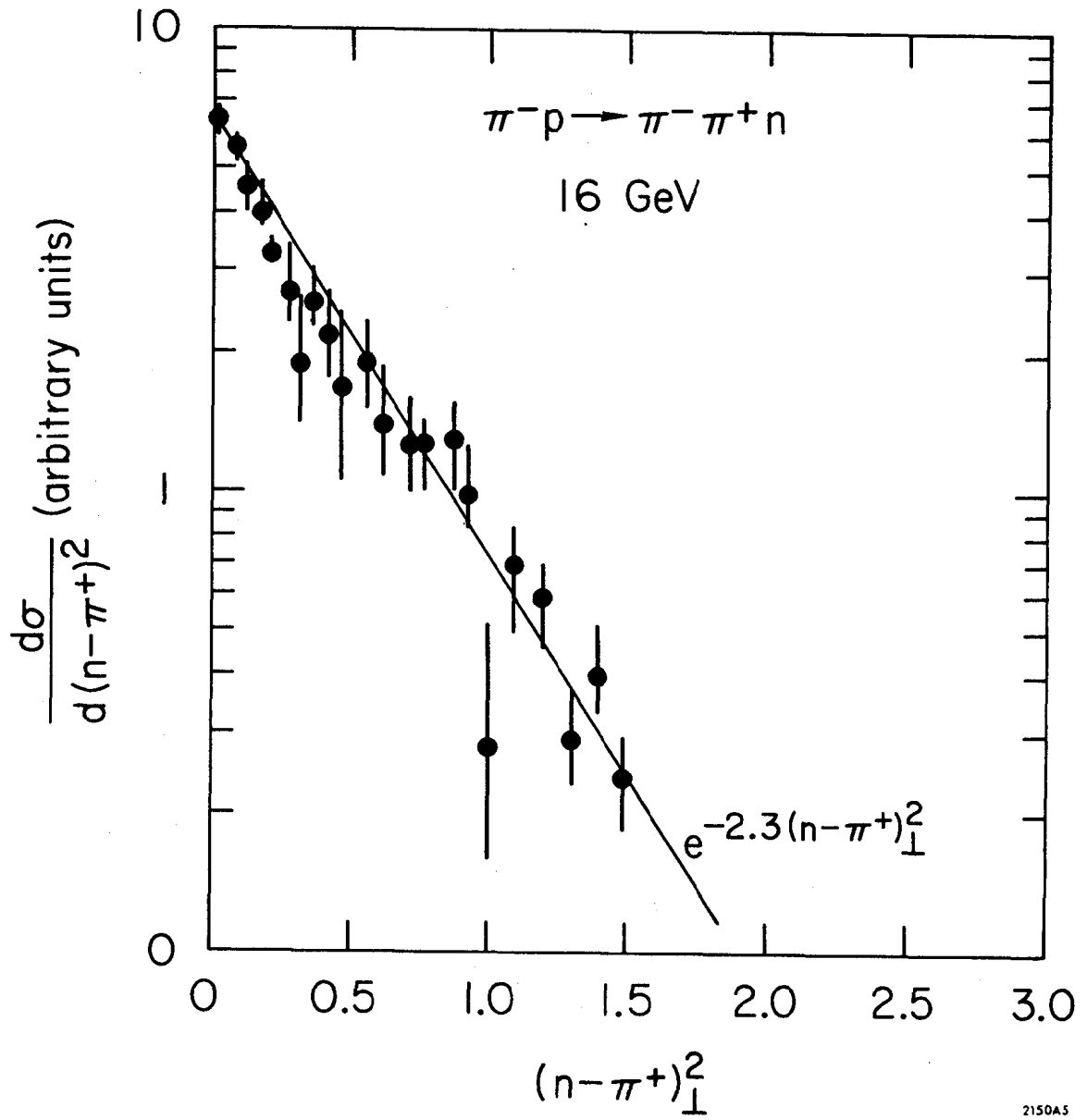


Fig. 14



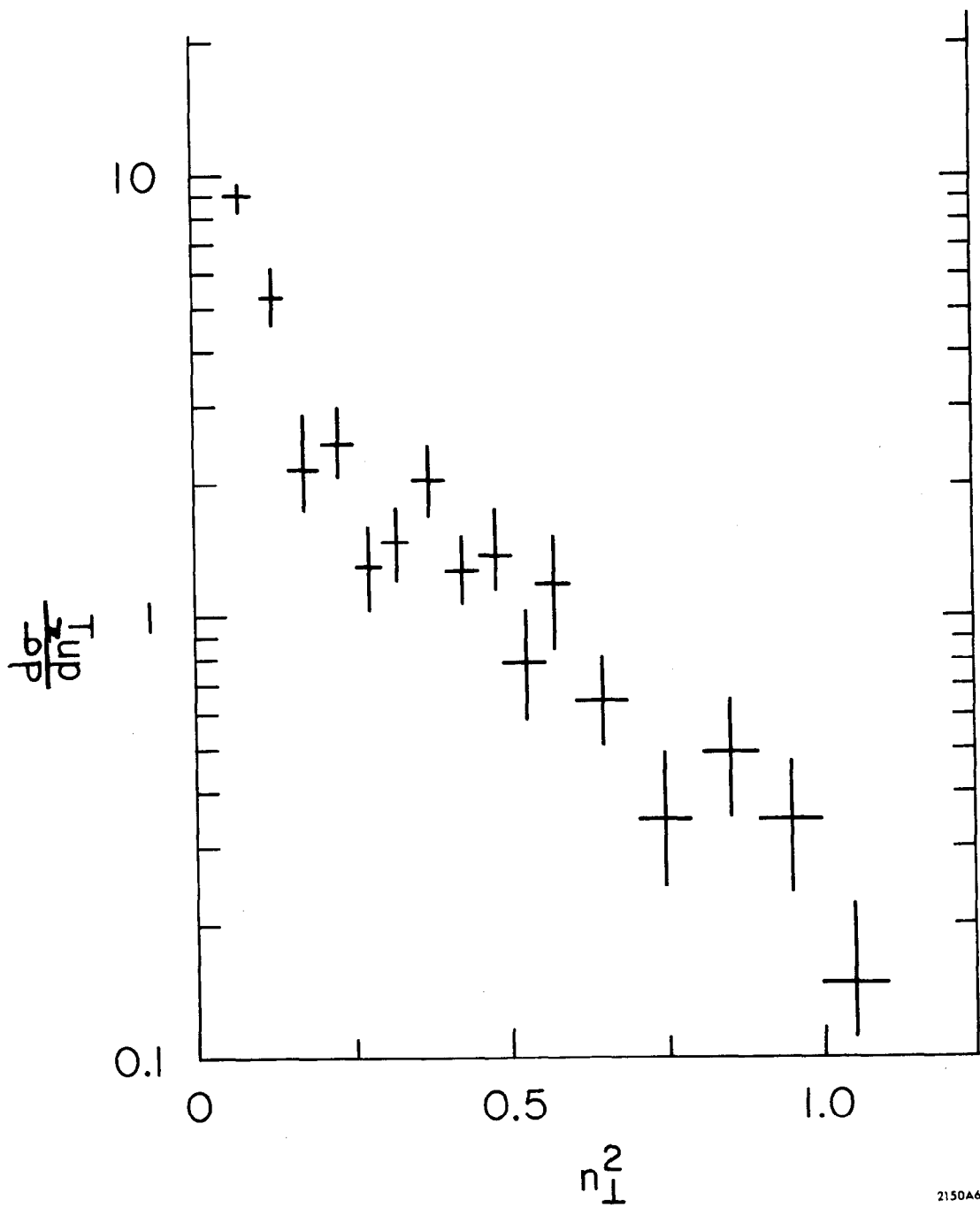
2150A4

Fig. 15a



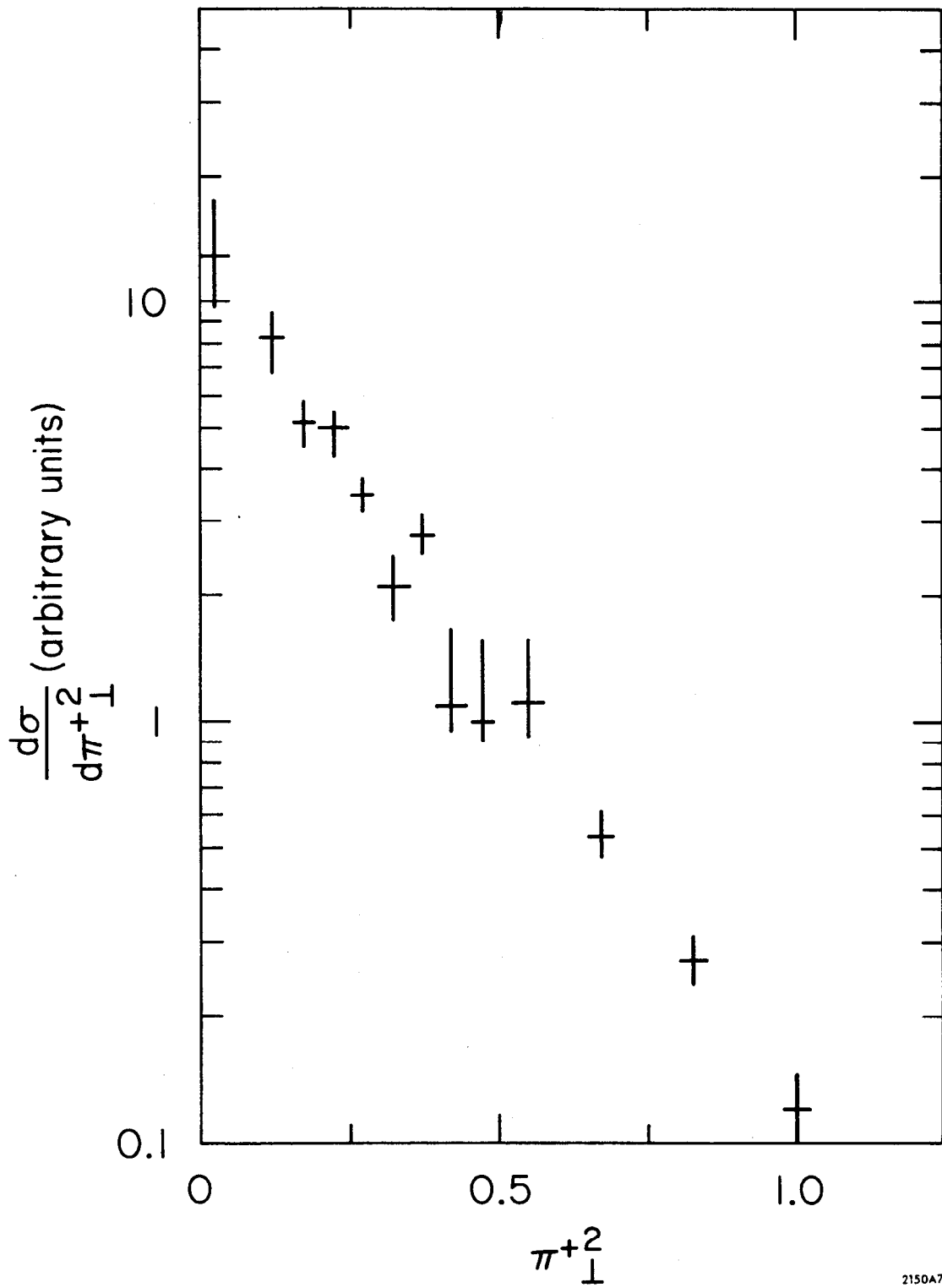
2150A5

Fig. 15b



2150A6

Fig. 15c



2150A7

Fig. 15d

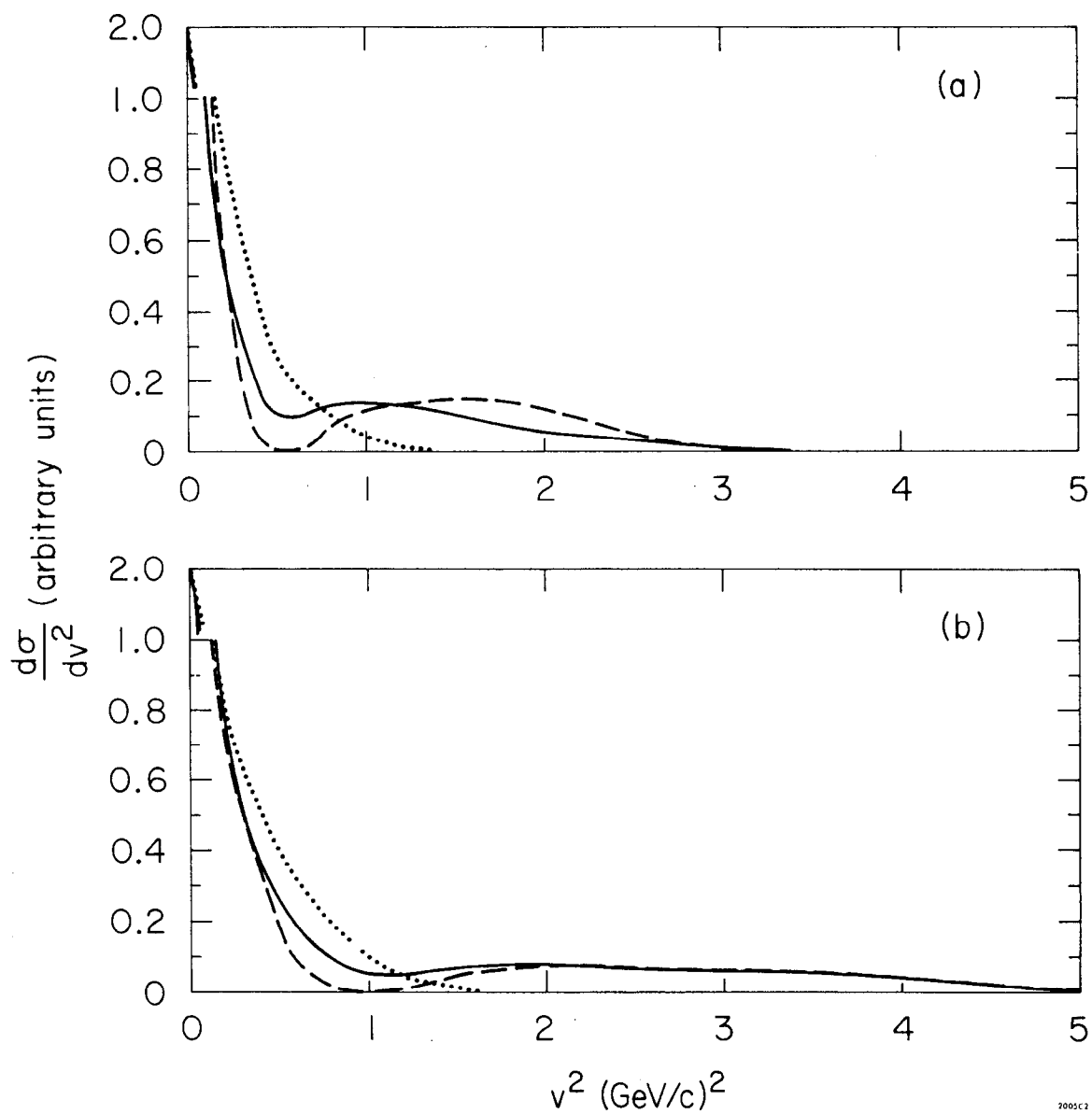
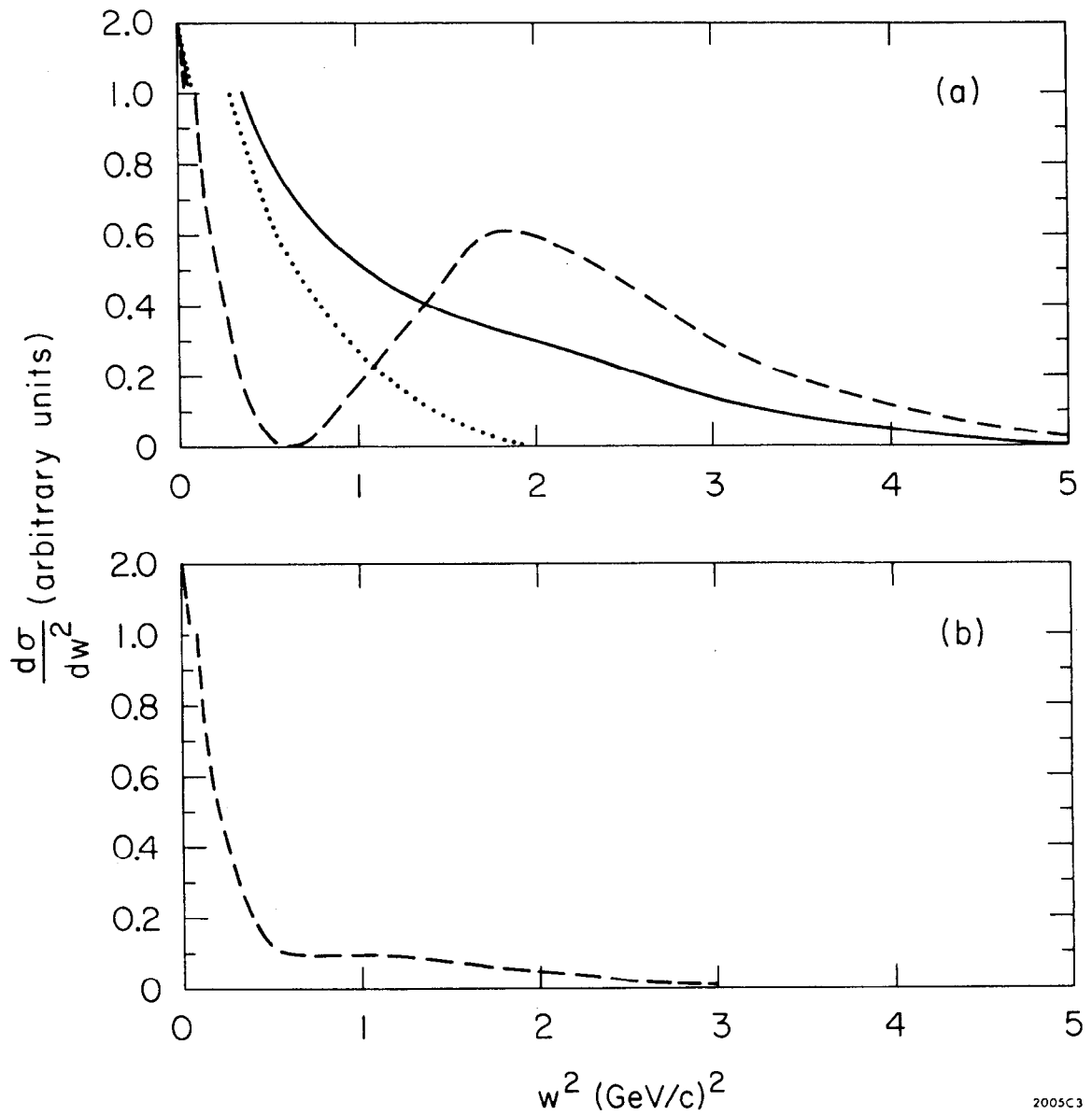


Fig. 16



2005C3

Fig. 17

(albeit roughly) it was necessary to modify phase space only slightly. Changing one of the momentum transfer Gaussians from  $k_{i\perp}^2$  to  $-t_i$  introduced sufficient energy dependence. The angular distributions were fit when the absorptive effects were introduced. These distributions will be discussed in greater detail below.

The striking feature is the long tail of events at large  $v^2$ . The simple theoretical parametrization used here should not be considered a fit to the data but the qualitative agreement is remarkable. The dotted line in fig. 16 is the distribution with no absorption ( $\lambda \equiv \epsilon = 0$ ) while the dashed line is that with  $\lambda = 1.5$ . The latter curve has a strong dip at  $v^2 \approx 0.50$ . This dip is due to the particular form assumed for the absorptive factor and is a common feature of the usual absorptive prescription. These dips will not appear if there are sufficient incoherent contributions to the cross section (e.g. helicity flip processes) to fill them. This effect can be studied by changing the energy. Another possibility is that neglected real parts in the subamplitudes and in the elastic rescattering will fill the dips. We saw earlier how complex absorption may affect real and imaginary parts differently. It is

actually sufficient, however, to make just the absorption complex. The result of the choice  $\text{Re } \lambda = 0.5$  and  $\text{Im } \lambda = 1.5$  (corresponding to  $\text{Re} T_{\alpha} / \text{Im} T_{\alpha} = 0.3$ ) is shown as the solid curve in fig. 16a. This curve is quite close to the data.

It is common in multi-Regge fits to change the slopes of the residues with the  $t_i$  to correspond to the experimental fact that two-particle amplitudes display much smaller  $t$ -slopes for large  $|t|$  than for small values of  $|t|$ . From our point of view, part of this is due to absorptive (both rescattering and production shadow) effects at large momentum transfers. One might believe that the broadening of the  $v^2$ -distribution could be accounted for by this effect alone but explicit computation, with no absorption and with sums of Gaussians (the tails of the two particle subamplitudes being of the form  $\exp(2.5t_i)$ ) shows that this is not the case. The reason is that the tails average away in the relative transverse momentum distributions. Strong absorption weights particular relative orientations of the subamplitude momentum transfers and thus enhances the large  $v^2$  region relative to the rest of the distribution.

We have computed the distributions for  $N=2$ , ( $\pi^+ p \rightarrow \pi^+ \pi^- \pi^+ p$ ), with the same parameters as above. The

distributions are shown in fig. 16b. Monte Carlo computation time limits further extension in multiplicity.

In the multiperipheral model one has assumed that rescattering is elastic. At small impact parameters however one might believe that rescattering is likely to be accompanied by production. For contrast we take an extreme view of this possibility in constructing the eikonal model of fig. 13b. Here, all production is an iterative process in the direct channel. The illustrated graph is eikonal in that it represents all Feynman (or Reggeon) graphs with all possible crossings of the vertical exchanges. The amplitude may be written as

$$M_N \propto \left(\frac{i}{2s}\right)^{N-1} \int d^2B S(B) \prod_{j=1}^N \left[ \int d^2b_j T_j(s_j, b_j) \widehat{T}_j\left(\frac{s}{s_j}, B-b_j\right) \cdot e^{i\vec{k}_j \cdot \vec{b}_j + i(\vec{k}_j + \vec{p}_j) \cdot (B-b_j)} \right]^{6.25}$$

The factor of  $(i/2s)$  accounts for the eikonal propagation of the outside particles between emissions. The energy factors associated with the couplings of the exchanges to the outside lines are included in the T-matrices. The quantity  $S(B)$  again represents absorption between the outside leading particles, reflecting elastic rescattering and the presence of

competing inelastic mechanisms at small impact parameters. Note that this is basically a model for pionization .

Since this model is not as familiar as the more common multiperipheral models it is useful to consider some of its global features. Since more exchanges occur ( $2N$ ) in this model than in the M.R. model ( $N+1$ ), for a given multiplicity, one might expect, unless one has Pomeron everywhere, that the M.R. mechanism would have the leading energy behaviour. This may be wrong for (at least) two reasons. First, as we have seen, contributions of the M.R. region may be strongly damped by absorption. Second, it may be possible to arrange phases and couplings such that some polyperipheral amplitudes will cancel some M.R. amplitudes.

The subamplitudes and absorptive factor will have the same form as in the previous model. All radii are taken equal ( $r^2=R^2$ ) since the distinction between geometrical and Regge choices is not as extreme as before. The transverse momentum conjugate to  $\vec{B}$  is just  $\vec{w}=\vec{k}-\vec{n}$ . The vector  $\vec{B}$  is now independent (the set of  $N+1$  vectors  $\langle \vec{B}, \vec{b}_j \rangle$  is then complete). For a given multiplicity  $N$ , the distribution in  $w^2$  is given by

$$\frac{d\sigma^{(N)}}{dw^2} = e^{-\frac{R^2 w^2}{2N}} \cdot \left[ 1 - \frac{\lambda}{1+2N} e^{\frac{R^2 w^2}{2N(N+2)}} \right]^2 \quad 6.26$$

with the same neglect of energy conservation as above. This expression is strikingly similar to that of the M.R. model in the case  $r^2=R^2/(N+1)$  but quite different from the same model with  $r^2=R^2$  (where in all models  $R^2$  may go like  $\ln s$ ). For fixed  $R^2$  the iterative model (like the first M.R.) predicts a broadening  $w^2$ -distribution as  $N$  increases and also a stronger absorptive effect because of the extra factor of  $1/(N+2)$  in the absorptive slope. The latter reduces the number of events in the intermediate  $w^2$  region and enhances the large  $w^2$  region. The distribution does not appear to be as broad as the Born terms would indicate, but it has a longer tail. These effects are all visible in the Monte Carlo predictions for the case  $N=2$ , shown in fig. 17a. The predictions of the multiperipheral model (with  $r^2=R^2$ ) for this distribution are shown in fig. 17b.

The distribution in the transverse momentum of an outside (leading) particle in this model is

$$\frac{d\sigma^{(N)}}{dk_{\perp}^2} = e^{-\frac{R^2 k_{\perp}^2}{N}} \cdot \left[ 1 - \frac{4\lambda N}{2N+3} e^{\frac{R^2 k_{\perp}^2}{N(2N+3)}} + \frac{\lambda^2 N^2}{(N+1)(N+2)} e^{\frac{R^2 k_{\perp}^2}{N(N+1)}} \right] \quad 6.27$$

Again, this is very similar to the M.R. result when  $r^2 = R^2(N+1)$  (equation 6.24). If  $R^2$  is constant, the distribution broadens with increasing multiplicity but the absorption enters with greater vigour at higher multiplicities. If  $R^2 \approx \langle N \rangle \approx \ln s$ , then the basic forward slope will not change, but the effect of absorption will change with  $N$ . In general, one expects  $R^2$  to have a part which is independent of  $s$  and a part which grows with  $s$ . If this is the case and  $N$  goes approximately as  $\ln s$ , then with no absorption, the forward peak will broaden with increasing  $s$ . However, absorption shrinks the peak by removing events from the moderate  $p_{\perp}^2$  region, in effect putting them into the larger transverse momentum region.

In the absence of constraints, the multiperipheral model represents a random walk in transverse configuration space. The step length is either constant ( $r^2 = R^2$  case), or varies with the local subenergy (as in our parton model). In contrast, the outside particles in the iterative production model undergo a random walk in transverse momentum space, in the absence of absorption. Absorption, which constrains walks in both spaces, forces models which appear very different to yield similar distributions. The close connection between the M.R.



mechanism (with  $r^2 = R^2/(N+1)$ ) and the polyperipheral models might imply that they should be treated equally in writing production amplitudes. Indeed, with couplings suitably chosen, and using M.R. phase space, it is possible to show that the graphs of fig. 18 cancel.<sup>35</sup> We thus have two choices, consider both mechanisms on the same footing, taking such cancellations into account, or absorb either mechanism and ignore the other. The distributions resulting from the latter choice are comfortingly similar. All of this should have been expected from our Born graph arguments for strong absorption. The M.R. is a competing mechanism for the iterative Born term and vice versa. The cancellation of the two kinds of amplitudes which can occur in the multi-Regge region is responsible for the vanishing of the absorptive factor in the M.R. amplitude of equation 6.17 when the strong absorption parameter  $\lambda$  reaches two.

The absorptive damping of the multi-Regge region in these models makes it useful to construct a fragmentation model in which more dynamical weight can be given to other regions of phase space. In particular, the secondaries can share larger fractions of the longitudinal momentum of the incoming particle. The absorptive effects come from the eikonal

rescattering which becomes strongly absorptive at small total impact parameters, as discussed in connection with the parton model.

Consider the case in which only one particle, of momentum  $P$ , fragments into  $N$  particles of longitudinal fractions  $y_i$  and transverse configuration space position  $x_i$ . This will be described by a wave function  $\Psi(\langle y_i, x_i \rangle)$  giving the amplitude for finding this configuration. The center of mass of the right moving cluster will be defined as

$$\vec{X}_{cm\perp} \equiv \sum_{i=1}^N y_i \vec{x}_{i\perp} \quad , \quad \sum_{i=1}^N y_i = 1 \quad 6.28$$

so that the transverse center of mass is nearest the fastest partons. The position of each parton relative to the cluster c.m. is  $\vec{r}_i = \vec{x}_i - \vec{X}_{cm}$  so that  $\sum y_i \vec{r}_i = 0$ . The relative transverse momentum conjugate to  $\vec{r}_i, -\vec{r}_j$  is  $\frac{y_j \vec{p}_i - y_i \vec{p}_j}{y_i + y_j}$ . Let the undissociating left-moving particle have coordinate  $Y$  and define  $\vec{B} = \vec{X}_{cm} - Y$ . Suppose the incoming particle (bound state) scatters according to  $A(B)$  and that the final constituents scatter according to  $\mathcal{P}_i(\vec{r}_i + \vec{B})$ , independently of the energies (as in the vector exchange eikonal model). With the momentum transfer  $\vec{\Delta}_\perp$  purely transverse, the general amplitude is

$$M_N = \int d^3B e^{iB \cdot \Delta} A(B) \prod_{i=1}^N \left[ \int d\vec{r}_i e^{i\vec{p}_i \cdot \vec{r}_i} \mathcal{O}_i(\vec{r}_i + \vec{B}) \right] \Psi(\langle \gamma_i, \vec{r}_i \rangle) \delta^2(\langle \gamma_i, \vec{r}_i \rangle)$$

6.29

There are a number of interesting cases to consider. There may be no initial state scattering so that  $A(B)=1$  (e.g.,  $\gamma p \rightarrow 2n\pi + p$ ). Or there may be only  $A(B)=1$  and  $\mathcal{O}=1$  (diffraction dissociation with no rescattering). The spatial dependence of the wave function may be unknown but for this picture to be reasonable its spatial range should be less than that of the exchange mechanisms. What we would like to determine are the experimental variables which most accurately probe the various dynamical mechanisms.

To do this, let us for simplicity restrict  $N$  to be 2 and let  $\Psi = \Psi(\vec{r}_1 - \vec{r}_2)$ . Choose  $\vec{r} \equiv \vec{r}_1 - \vec{r}_2$  so that, with the delta function,  $\vec{r}_1 = y_2 \vec{r}$  and  $\vec{r}_2 = -y_1 \vec{r}$ . The configuration is as in fig. 19.

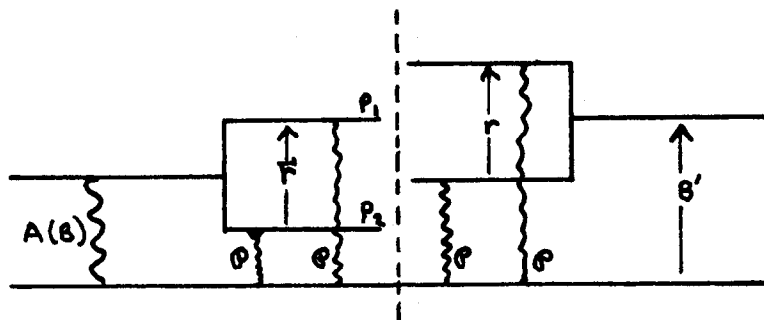


Fig. 19

The amplitude has the form

$$M_{2 \rightarrow 3} = \int d^3 B e^{i B \cdot \Delta} A(B) \int d^3 r e^{i p \cdot r} \Psi_Y(r) \mathcal{O}_1(B + Y_2 r) \mathcal{O}_2(B - Y_1 r) \quad 6.30$$

where  $\vec{p} \equiv y_2 \vec{p}_1 - y_1 \vec{p}_2$  ( $y_1 + y_2 = 1$ ) is the relative momentum.

Holding longitudinal variables fixed (the differential volume element being  $d^2 p_L$ ), the distribution in the momentum transfer  $\vec{\Delta}$  is

$$\begin{aligned} \frac{d\sigma}{d\Delta^2 d^2 p_L} &= \int d^2 B' d^2 B e^{i \Delta \cdot (B - B')} A^*(B') A(B) \cdot \\ &\cdot \int d^3 r |\Psi(r)|^2 \mathcal{O}_1^*(B + Y_2 r) \mathcal{O}_2^*(B' - Y_1 r) \mathcal{O}_1(B + Y_2 r) \mathcal{O}_2(B - Y_1 r) \end{aligned} \quad 6.31$$

If  $|\Psi(r)|^2 = c f(y_i) \delta^2(r)$ , then we immediately have

$$\frac{d\sigma}{d\Delta^2 d^2 p_L} = c f(y_i) \left| \int d^2 B e^{i \Delta \cdot B} A(B) \mathcal{O}(B + Y_2 r) \mathcal{O}(B - Y_1 r) \right|^2 \quad 6.32$$

so that the distribution in  $\Delta$  is sensitive to all the scattering, as we would expect. This will hold even if  $\Psi$  is broad in configuration space unless the functions  $\mathcal{O}$  vary rapidly with transverse argument.

The distribution in the variable  $\vec{v} \equiv \vec{p}_1 - \vec{q} = \vec{p} + (1 + y_1) \vec{\Delta}$  is given by

$$\frac{d\sigma}{dv^2 d\rho_L} = \int d^2u d^2u' \rho_1^*(2u') \rho_1(2u) e^{i v \cdot (u-u')} \cdot$$

$$\cdot \int d^2w A^*(\gamma_2 w + (1+\gamma_1)u) A(\gamma_2 w + (1+\gamma_1)u)$$

$$\cdot \Psi^*(u'-w) \Psi(u-w) \rho_2^*(u'+w) \rho_2(u+w) \quad 6.33$$

For  $\gamma_2 \neq 0$ , the integration over  $w$  tends to average the effects of the dynamical mechanisms  $A$ ,  $\Psi$ , and  $\rho_2$ , so that the distribution in  $v^2$  (the relative momentum of constituent one and the other particle), reflects most directly the effect of scattering between these particles. If  $\gamma_2 = 0$ , so that  $\gamma_1 = 1$ , then constituent one is the center of mass (by our definition) and the distribution also reflects the initial state scattering  $A$ .  $\Psi$  itself determines how likely it is that  $\gamma_2 = 0$ . If the wave function is very short range, then the  $v^2$ -distribution also reflects the other interactions.

The distribution in the relative momentum between the two constituents is

$$\frac{d\sigma}{dP^2 d\rho_L} = \int d^2r d^2r' \Psi^*(r') \Psi(r) e^{i P \cdot (r-r')} \int d^2B |A(B)|^2 \cdot$$

$$\cdot \rho_1^*(B+\gamma_2 r') \rho_2^*(B-\gamma_1 r) \rho_1(B+\gamma_2 r) \rho_2(B-\gamma_1 r) \quad 6.34$$

As one would expect, this distribution most clearly measures the wave function. If  $\Psi$  is very narrow in  $r$ , large values of  $P$  are possible.

The example above is somewhat trivial since the number of secondaries is small, but the same principles apply in the more complicated cases. Several general conclusions may be drawn. If the transverse size of the wave function is less than the range of the exchange mechanisms, the the slope of the distribution in  $p^2$  should be less than the slope of the distribution in  $\Delta^2$ . Furthermore, when we compare the relative momentum distribution of two right-movers with that of a right-mover and a left-mover ( $\vec{v}$ ), the latter should be steeper and demonstrate absorptive breaks and a tail, as in the previous models. The rescattering effects within a right-moving cluster are so numerous and random in direction that no breaks or broadening should be apparent there. These effects are shown in fig. 20.

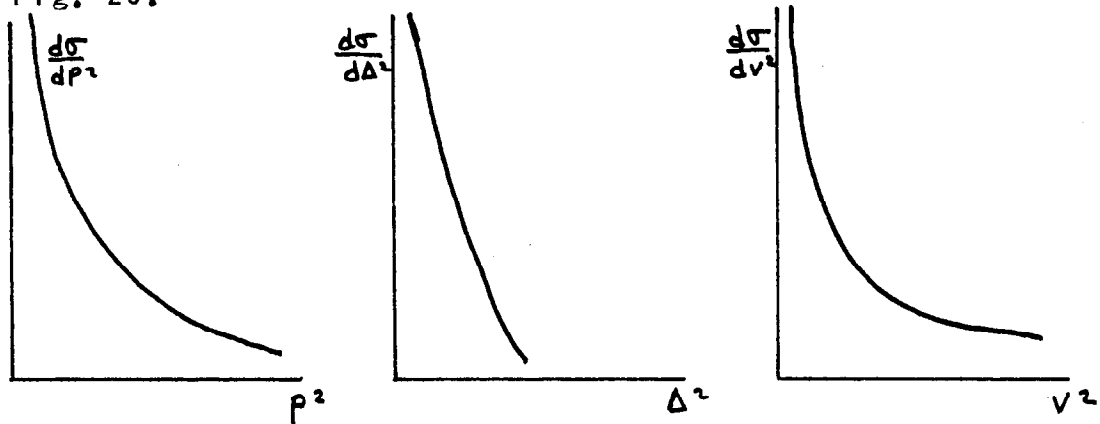


Fig. 20

The break in the  $v^2$  distribution may be much sharper here than that predicted by the M.R. model.

## VII. AZIMUTHAL DISTRIBUTIONS AND THE GEOMETRY OF PRODUCTION

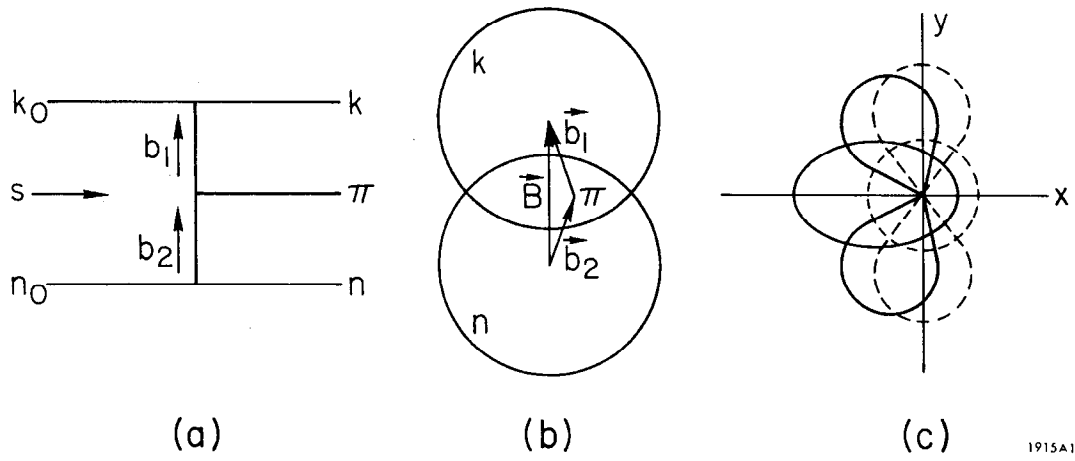
We have thus far avoided treating the more conventional approach to two-particle correlations in the form of azimuthal distributions. As mentioned in the introduction, it is necessary to separate the effects of momentum conservation, which implies that as soon as one selects a particle moving in a particular transverse direction, the second particle selected from the same event is most likely moving in some other direction. If  $\phi$  is the relative angle between the two transverse momentum vectors, the distribution in  $\phi$  will tend to have an asymmetry with a peak at  $\phi = \pi$ . The occurrence of dynamically induced correlations thus reduces to a question of the quantitative magnitude of the asymmetry. The small effects discussed above in which events with moderate values of relative transverse momentum are reduced in number while those with larger values are made more numerous will tend to increase the azimuthal asymmetry, but not dramatically.

However, these distributions, and the cartesian distributions introduced below, can be very useful and revealing. In particular, the point of view

associated with these distributions may allow a more direct geometrical interpretation, in the spirit of Yang and coworkers, of production mechanisms.

We first call attention to the fact, elaborated below, that it is difficult to make any factorizable model for production produce azimuthal distributions with sufficient assymetry to fit the data. This would be true even if these distributions were fit entirely by phase space. A factorizable model results in sufficient distortion of phase space to make this true. An example is the two-fireball model of the introduction. The multi-Regge model also has this effect since the ordering of the chain implies that all final state momenta are not cut off in the same way. This example will be returned to below. Note, however, that if sufficient M.R. configurations contribute then this effect may be reduced. The important point is that model assumptions must be made to cut off the transverse spectra. How this is done has a great influence on the resulting azimuthal distributions.

Consider the  $2 \rightarrow 3$  multiperipheral amplitude of equation 6.1. The notation is as in fig. 21a, where the geometry in transverse configuration space is shown in fig. 21b. One can interpret this picture as the overlap of two extended hadrons with production



1915A1

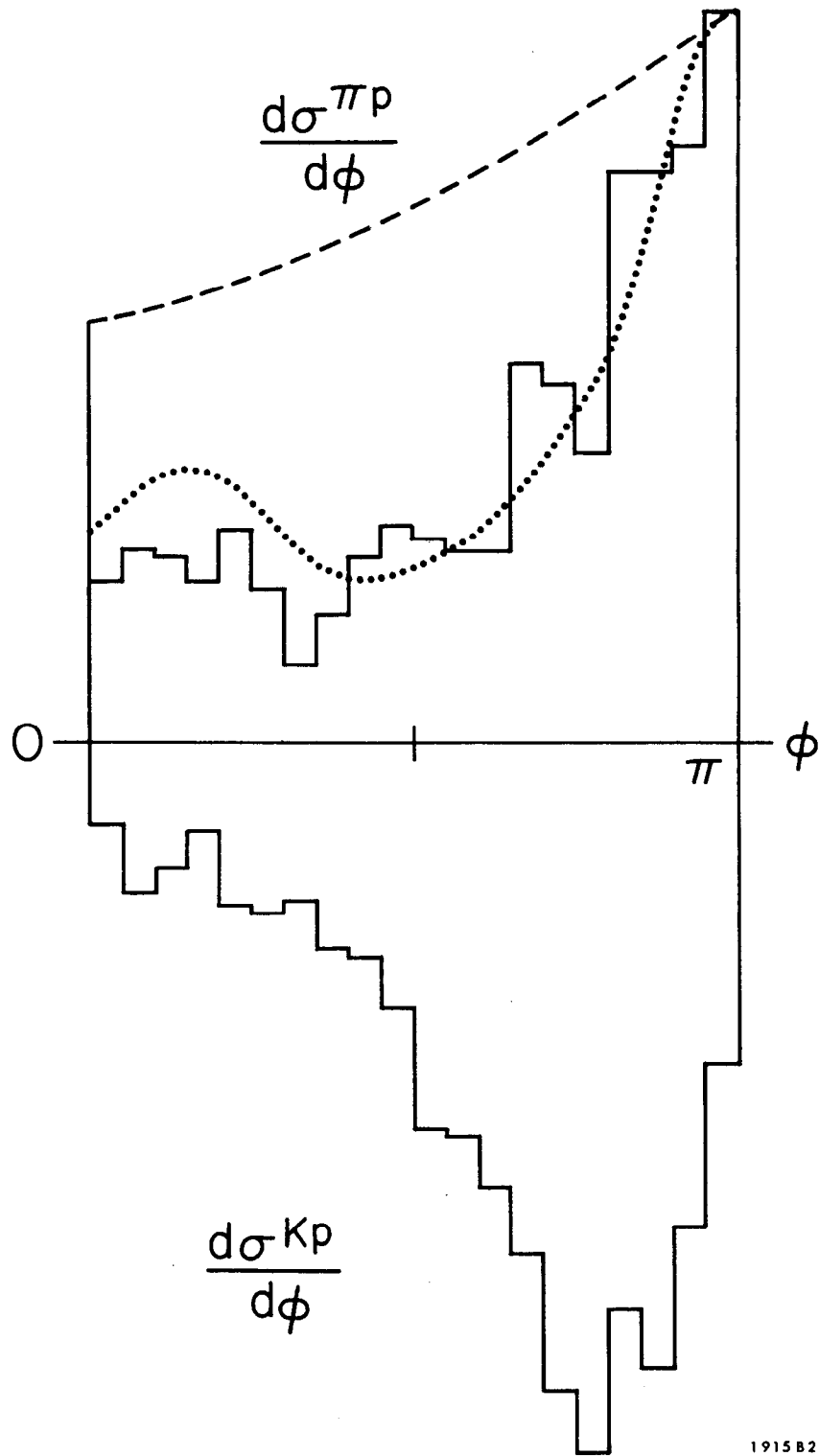
Fig. 21

resulting from the overlap region. For experimental convenience one can parametrize the distributions in transverse momenta in the simple form

$$G(\vec{k}, \vec{n}) = G_0 e^{-a\vec{k}_\perp^2 - b\vec{n}_\perp^2 - c\vec{k}_\perp \cdot \vec{n}_\perp} \Phi(k, n, s) \quad 7.1$$

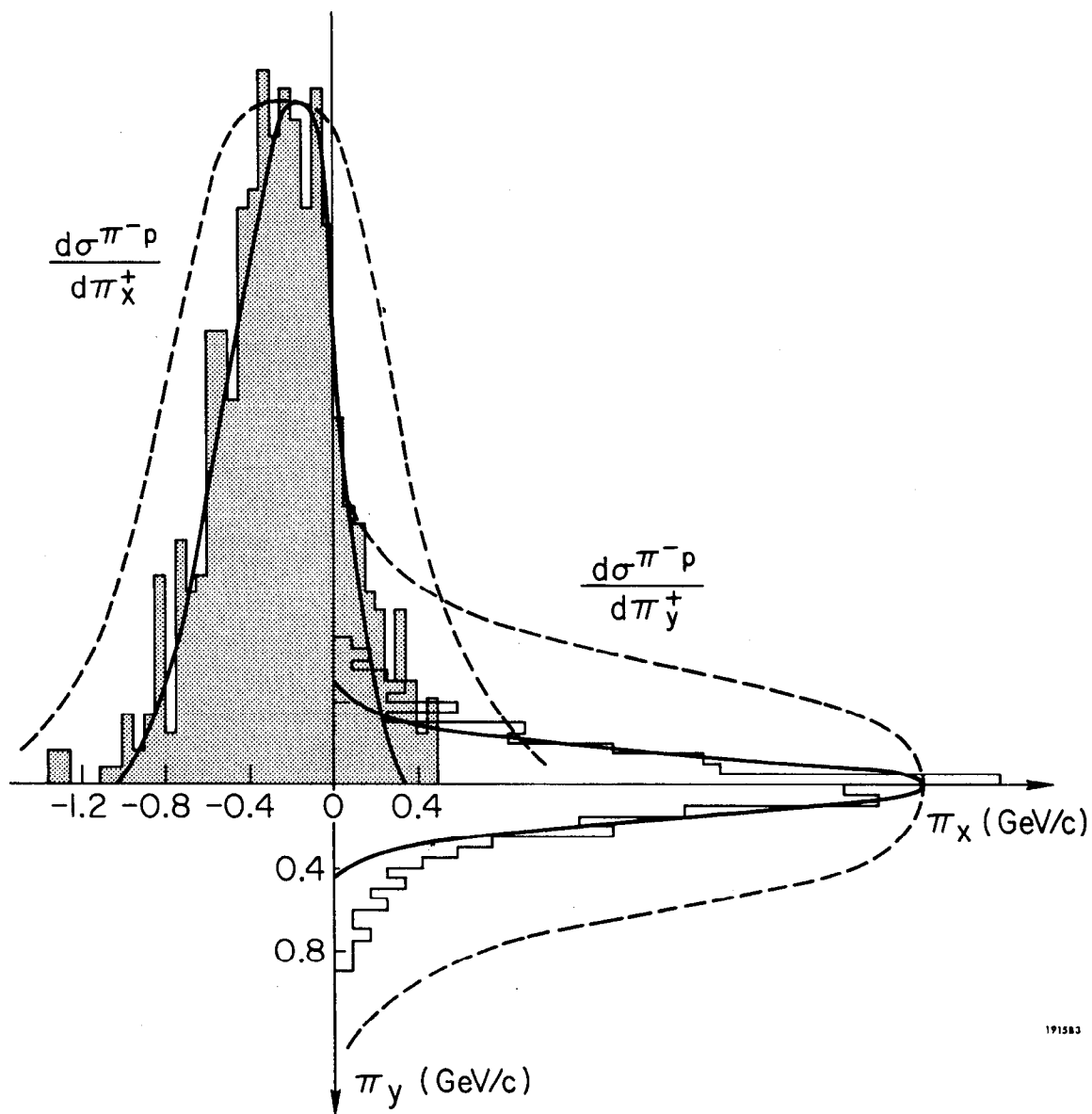
where  $\vec{k}_\perp$  and  $\vec{n}_\perp$  are the transverse momenta of the two leading final state particles. Note that the simple multiperipheral model would have the parameter  $c=0$ . In comparing with experiment more precisely, the full absorptive results should be used. The phenomenological form is useful for locating model dependent assymetries.

The experimental results for the azimuthal distribution between leading boson and leading baryon in the reaction  $\pi^- p \rightarrow \pi^- \pi^+ n$  at 16 GeV/c are shown in fig. 22a. The dashed line is a best fit with  $c=0$ , demonstrating that the simple multiperipheral model is incapable of fitting the distribution. The dotted line is the absorptive model prediction. The radius of the  $\pi\pi$  subamplitude was taken as  $R^2=6$ , that of the  $\pi-p$  subamplitude as  $R^2=11$ , and that of the absorptive factor as  $R^2=8$ . The latter were rough fits to the  $\pi p$  quasi-elastic and elastic t-distributions. The radius



191582

Fig. 22a



191583

Fig. 22b

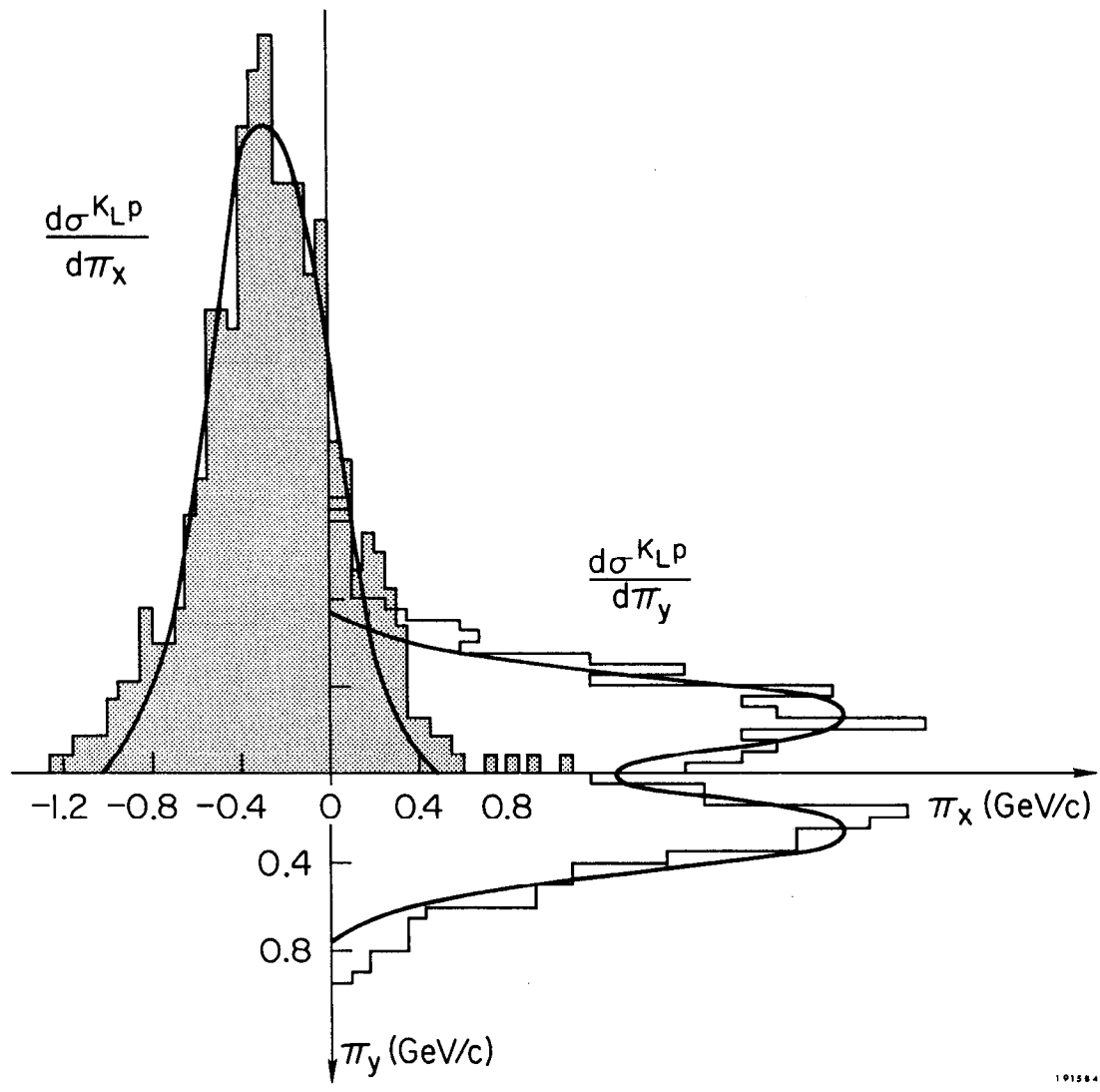


Fig. 22c

is about what one would expect from a quark model. It is interesting to note that the bump near  $\phi = 0$  is given by the absorptive prescription. There is a correspondingly striking effect upon the leading particle transverse momentum distributions. With this parametrization there should be a break in the transverse momentum spectrum of the leading nucleon at about  $P_{\perp}^2 = 0.25$ . This should be compared with the data of fig. 15c.

One can also plot the data as cartesian correlations. Choose a leading particle transverse momentum vector to fix the the x-axis. Then project the the transverse momentum of the produced secondary onto this and the orthogonal y-axis. The resulting distributions are shown in fig. 22b. These are the projections of the radiation patterns shown in fig. 21c. The prediction of pure phase space for the  $\pi p$  reaction is shown as the dotted line. Note that this demonstrates the negative azimuthal correlation due to momentum conservation, in shifting the x-distribution to the left. The solid curve is a rough fit with the phenomenological parametrization with  $a=4$ ,  $b=12$ , and  $c=6$ . The parameter  $c$  is related to the magnitude of the absorptive radius. It is interesting to note that it is of the same order as the other parameters.

The introduction of spin has very interesting consequences in this picture. To see this we consider the pair of reactions



where in the multiperipheral model of fig. 21a, there are contributions from both pion and omega exchange. In the latter case, we must couple two vectors to a pseudoscalar at the central vertex. We could proceed in configuration space where, as pointed out earlier the spin couplings are sensitive to the directions of the impact parameters and may be written as gradients in momentum space. It is easier here to proceed by writing down the only possible form. The spin couplings will be taken to be multiplicative (note that in Toller analysis the effect of  $m \neq 0$  couplings is also multiplicative and does not appear in the exponentials). The simplest generalization of the phenomenological parametrization is

$$G(\vec{k}, \vec{k}') = \left[ g_0 e^{-b_0 \vec{n}^2} + g_1 a b_1 \left\{ (\hat{z} \wedge \vec{k}) \cdot \vec{\pi} \right\}^2 e^{-b_1 \vec{n}^2} \right] e^{-a \vec{k}^2 - c \vec{n} \cdot \vec{k}} \quad 7.3$$

We shall interpret the pion exchange contribution as transverse monopole radiation and that due to vector exchange as dipole radiation. These labels have more than mnemonic value as may be seen

from fig. 22c, where data from the two kaon reactions for events with invariant masses (subenergies) above the  $K^*$  and  $\Delta$  resonance regions is presented. The effects of both monopole and dipole radiation are visible. A good fit, depending only slightly upon invariant masses, is obtained with  $a=6, b_0=b_1=10, c=6,$  and  $g_0/g_1=7.4$ . The important point is that the monopole and dipole contributions appear to have the same exponential dependence. The parameters vary over the mass ranges, most strongly in the resonance regions, but seem to approach asymptotic values at high subenergies. The dipole term tends to dominate the  $K^*$  resonance region, the relative weights changing as one moves through it. The azimuthal correlation analysis provides a clear and intuitive way of studying this region.

## VIII. CONCLUSION

The general problem of constructing hadronic multiparticle amplitudes is as yet unsolved. Although it is not a priori obvious, it would be extremely convenient if this task required only knowledge of the amplitudes involved in two-body and quasi-two-body reactions--reactions which have been extensively studied and parametrized. This assumption underlies all contemporary models for multiparticle amplitudes,, but the complexity of the problem requires further strong assumptions about the way in which two-body singularities are utilized. Because of factorization properties or similar statistical assumptions, these models produce average or global distributions which reflect primarily these statistical properties. It would be useful to consider how more detailed tests might be made and to consider how even the usual factorization assumptions may be incorrect at the local dynamical level at which they are imposed.

An important constraint on the construction of multiparticle amplitudes is that of full  $n \rightarrow m$  body unitarity. In this connection, we have suggested that the choice of a particular Born term for production, built from two-body (perhaps off energy or angular

momentum shell) amplitudes, is not without hazards. First, it may not incorporate initial and final state interactions (initial and final being defined by the Born term) or absorptive effects. The multiperipheral model is particularly vulnerable here. Even the possibility that the hadronic force is vector in character and that the impulse and not the time for rescattering is important makes momentum space factorization arguments suspect. Second, the assumed Born term may not incorporate all the production dynamics (particularly at small distances), leading the necessity for strong absorption, as discussed in section II.

This suggests that the existence of many-body degrees of freedom is an essential problem in production. The parton model construction introduced in section III indicates, albeit in heuristic fashion, how this may come about when considered from both Regge and eikonal points of view. New cuts appear in the former at the level of small distance (or large momentum) structure and corrections must be made in the eikonal treatment. The fact that the Regge view more properly treats the large configuration space or small momentum space dynamics while the eikonal connects regions far apart in momentum space and is more

intimately connected with s-channel unitarity makes these approaches highly complementary. Absorption results. The small distance dynamics, leading to corrections to both pictures (for the eikonal, these are configuration space gradients), implies the necessity for strong absorption (for which we have only an ad hoc prescription), altering the original description of, for example, intermediate transverse momentum regions and emphasizing the role of the large momentum region. The preliminary ISR data suggest that this region is far richer dynamically than most had thought.

The parton model construction indicates the general features of this problem but it is only in the model constructions that one can deduce the variables appropriate to testing specific local dynamical assumptions. The fact that absorption of very different mechanisms leads to very similar distributions in these new variables does not inspire confidence that any particularly simple choice of local dynamics is correct. The experimental evidence begins to suggest that one must look for clues in effects involving only a small percentage of the data. One suspects that it will be difficult to find definitive evidence for any particular dynamical mechanism for production. There

is thus no conclusion, unless one is willing to accept  
that of Samuel Beckett:<sup>36</sup>

Remember there is no triangle, however  
obtuse, but the circumference of some  
circle passes through its wretched  
vertices.

## REFERENCES

1. J. Finkelstein and K. Kajantie, Phys. Lett. B26, 305 (1968) and many subsequent rediscoveries.
2. H. Harari and A. Schwimmer, Phys. Rev. D5, 2780 (1972).
3. There is by now an immense literature. See K. Wilson, CLNS-131 (November, 1970, unpublished) and J. Ellis, J. Finkelstein and R. D. Peccei, SLAC-PUB-1020 (ITP-401).
4. One of the most complete developments of this analogy is M. Bander, University of California at Irvine preprint (71-33), "Multiparticle Production--Feynman Fluid Analogy."
5. C. E. DeTar, D. Z. Freedman and G. Veneziano, Phys. Rev. D4, 906 (1971).
6. I thank R. Sugar and J. Fulco for useful discussions regarding the following formalism. Similar attempts have recently been made by R. J. Yaes, Lett. Al Nuovo Cimento 4, 611 (1972) and J. Beaupre, Aachen preprint (April, 1972). The latter paper makes unrealistic factorization assumptions on the inclusive multiparticle distributions.
7. J. D. Bjorken and S. J. Brodsky, Phys. Rev. D1, 1416 (1970).
8. The way in which these functions differ in the fragmentation regions is model dependent only as a result of the energy normalization introduced through the choice of the function  $g(s)$ . There can be no fully model-independent correlation functions--all definitions involve dynamical assumptions.
9. S. Stone, T. Ferbel, P. Slattery, B. Werner, Rochester preprint UR 875-349 (April, 1972).
10. This representation is very ancient. See, for example, reference two above.
11. F. Henyey, G. L. Kane, J. Pumplin, and M. H. Ross, Phys. Rev. 182, 1579 (1969).

12. D. Amati, A. Stanghellini and S. Fubini, Nuovo Cimento 26, 896 (1962). and S. Mandelstam, Nuovo Cimento 30, 1113,1127,1148 (1963).
13. This parton cascade condition is suggested by J. Kogut and L. Susskind, IAS preprint (March, 1972). These authors develop a string model for hadrons, rather than for hadronic amplitudes. A crucial difference is that the wee regions are then associated with the individual hadrons.
14. R. P. Feynman, High Energy Collisions (Gordon and Breach, New York, 1969), p. 237.
15. For consistency we note this point of view naturally incorporates the usual picture of the electromagnetic properties of hadrons. The elastic form factor, for example, falls very rapidly for  $q^2$  small because it sees only the diffuse large-scale behaviour. As  $-q^2$  increases, the virtual photon probes into the charge density of the small scale region. The limited spatial support of this region means that the form factor falls much less rapidly in  $q^2$ . The deep-inelastic structure functions behave similarly except that in the Bjorken-Johnson-Low limit with the energy transfer  $\nu (=q \cdot p)$  large in addition to  $-q^2$ , the associated time is small. The deep inelastic photon attaches to partons with longitudinal fraction  $x = -q/2m\nu$ . These will be the "free" partons of the diffuse large-scale region. Since  $\nu$  is limited by  $\sqrt{s}$ , the wee region does not contribute. The region of large  $\nu/q^2$ , that is far out along the light-cone, defines the onset of the Regge contribution to deep-inelastic scattering. Absorptive effects, if they exist here, will break scaling.
16. E. Yen and E. L. Berger, Phys. Rev. Letters 24, 695 (1970).
17. The derivative  $\partial_- (=d/dx_-)$  samples the variation of the particle wave function away from the light cone  $x_- = 0$ .
18. S. J. Chang and T.-M. Yan, Phys. Rev. Letters 25, 1586 (1970).

19. G. Tiktopoulos and S. B. Treimam, Phys. Rev. D3, 1037 (1971).
20. If the single M-R. chain gives  $\ln s$  multiplicity then the effect of unitarization, as in our parton model, redistributes this multiplicity so as to enhance the low missing mass ( $M^2$ ) region over the M-R. prediction. The effect is thus in the right direction but the strength (the inverse power of  $M^2$ ) is undetermined just as we cannot see that the multiplicity need be precisely  $\ln s$ . In very different language the suppression of high mass diffractive states results from the vanishing of the triple-Pomeron coupling.
21. Chan Hong-Mo, J. Loskiewicz and W. W. M. Allison, Nuovo Cimento 57A, 93 (1968).
22. N. J. Sopkovich, Nuovo Cimento 26, 186 (1962).
23. K. Gottfried, J. D. Jackson, Nuovo Cimento 34, 735 (1964).
24. J. D. Jackson, Rev. Mod. Phys. 37, 484 (1965). and L. Durand and Y. T. Chiu, Phys. Rev. 139B, 646 (1965).
25. If it is assumed to be the correct amplitude, and not merely a high energy approximation, a real fixed pole on the physical sheet is prohibited by t-channel unitarity. See F. Zachariasen, Physics Reports 2C, vol. 1, 23 (1971).
26. J. Schwinger, unpublished lecture notes (1952); H. D. I. Abarbanel and C. Itzykson, Phys. Rev. Letters 23, 53 (1969).
27. M. Levy and J. Sucher, Phys. Rev. 186, 1656 (1969); R. Blankenbecler and R. L. Sugar, Phys. Rev. D2, 3024 (1970).
28. See, for example, N.-P. Chang, Phys. Rev. 172, 1796 (1968).
29. A more complete discussion of the transcription from helicity representation to impact representation is W. Drechsler, Fortschritte der Physik 18, 305-448 (1970) and Munich

preprint "Spin Structure of High Energy Multiple Scattering" (1971).

30. An example of this is Y. Avni, SLAC-PUB-1048 (May, 1972).
31. F. Halzen and C. Michael, Phys. Letters 36B, 367 (1971).
32. R. L. Thews, G. R. Goldstein and J. F. Owens III, Arizona preprint "A New Regge Absorption Model" (April, 1972).
33. There is a dynamical difference here. The dependence upon Toller  $m \neq 0$  quantum numbers in two-particle inclusive distributions calculated from the dual resonance model is in the form of a multiplicative coefficient function,  $\cos(m\phi)$ , where  $\phi$  is the angle between the adjacent momentum transfers in the secondaries rest frame. In our case similar spin coupling factors appear but the important azimuthal dependences in the total center of mass appear in the exponentials. See D. Freedman, E. Jones, F. Low, and J. Young, Phys. Rev. Letters 26, 1197 (1971); C. Jen, K. Kang, P. Shen and C.-I. Tan, Phys. Rev. Letters 27, 458 (1971).
34. I would like to express my thanks to K. Moriyasu and J. Loos and D. Leith, for their assistance and permission in analyzing the Group B data in terms of the somewhat unconventional variables presented here.
35. This cancellation has been demonstrated in the explicitly unitary model of R. Aviv, R. Blankenbecler and R. L. Sugar, Phys. Rev. D5, 3252 (1972).
36. Samuel Beckett, Murphy (Grove Press, Inc., 1962).